Scientific Research Publishing

Journal of High Energy Physics, Gravitation and Cosmology, 2026, 12(1), 169-223
https://www.scirp.org/journal/jhepgc
ISSN Online: 2380-4335
ISSN Print: 2380-4327

Could Tachyonic Magnetic Monopole Neutrinos Be the Fundamental Cause of Gravitational Phenomena in the Universe

Eue-Jin Jeong

Tachyonics Institute of Technology, Austin, TX, USA
Email: euejinjeong@utexas.edu

How to cite this paper: Jeong, E.-J. (2026) Could Tachyonic Magnetic Monopole Neutrinos Be the Fundamental Cause of Gravitational Phenomena in the Universe. *Journal of High Energy Physics, Gravitation and Cosmology*, **12**, 169-223.
https://doi.org/10.4236/jhepgc.2026.121012

Received: September 7, 2025
Accepted: January 4, 2026
Published: January 7, 2026

Abstract

Moving electrically charged particles create a spiraling magnetic field around them according to Maxwell's equation, and each hadron containing fractionally charged quarks will be filled with randomly fluctuating magnetic fields, which are known as quark gluon plasma that binds each hadron as a single particle. If we consider that neutrinos are magnetic monopole particles traveling at extremely high speeds, the chance of magnetic monopole neutrinos passing through the core of hadrons without interference will be extremely small. We theorize that inertia and gravity are caused by the impediment of the passage of the background magnetic monopole neutrinos by the hadronic matter particles, which causes local spatial density modification of the surrounding background neutrinos. Weak interactions manifest in the decay of a neutron into a proton and an electron, where the neutrino is emitted during the decay process to conserve energy and momentum. Therefore, in theory, there should be as many electron neutrinos as protons or electrons in the universe. The compelling question for physicists is where all those neutrinos are and what they contribute to the workings of the universe. Are they sitting idly doing nothing or actively participating in the universe's work? When it was generally concluded that neutrinos do not have either electric or magnetic charges, there are no neutrinos that can contribute to the workings of the universe within the known framework of particle interactions. In the hypothesis of tachyonic magnetic monopole background neutrinos, the mass of a particle is defined by how much resistance the particle experiences owing to the presence of fast-traveling tachyonic magnetic monopoles. Naturally, the heaviest matter causes the greatest obstruction to the passage of these neutrinos. Blackholes are gigantic quark gluon plasmas that obstruct the passage of background neutrinos in space, forming an impenetrable vacuum for these neutrinos. In effect, we can conceptually relate the effect of gravity to the magnetic

monopole property of the neutrinos interacting with the magnetic field of the gluons created by the fast-moving quarks inside the hadrons. The fundamental cause of gravity toward the center of mass of a massive gravitating object can be viewed as a result of the absence of background neutrinos coming from the direction of the gravitating object owing to the blockage of the neutrino particles. There is insufficient flux of neutrinos coming from the direction of the massive gravitating object to stop the pushing effect from the opposite side of the object. In an empty space, an isolated macroscopic object remains in the same position according to the principle of Newtonian mechanics, because the force produced by the impinging neutrino flux toward the object is homogenous and isotropic in all directions, and it does not cause the object to move toward any particular direction, which is essentially the manifestation of Newton's first law of motion.

Keywords

Gravity, Neutrinos, Tachyons, Magnetic Monopole, General Relativity, QCD, Quantum Field Theory

1. Introduction

In a recently published paper presented in Section 5, we report on the measured magnetic monopole charge of neutrons by observing the existence of the vertical component of the magnetic field in the equator of the Earth. Because the Earth's dipole magnetic field is parallel to the surface of the Earth on the equator, this non-zero component of the vertical magnetic field must originate from the magnetic monopole charge of the neutrons. Apart from the horizontal component of the Earth's dipole magnetic field, it is noticed that the magnetic compass tends to tilt vertically in the high latitude region of the Earth, either north or south. This is due to the curved shape of the dipole magnetic field of Earth. However, in the equatorial region, there should be no vertical component of the Earth's magnetic field because the Earth's dipole magnetic field runs horizontally in the equatorial region of the Earth, and if there is no magnetic monopole effect from all neutrons in the Earth. If there is any vertical component of the magnetic field in the equatorial region, it must be considered as coming from the magnetic monopole field caused by the massive number of neutrons on Earth. Based on experiments performed in Cuenca, Ecuador, and other areas of the equatorial region on Earth, we were able to determine the strength of the individual monopole magnetic charge of the neutrons. Consequently, because of the general charge conservation principle, this magnetic monopole charge of the neutron must be transferred to neutrinos in the process of nuclear beta decay, and we found that the background neutrinos have a very small amount of magnetic monopole charge of the north type, according to the precision measurement. In this paper, we demonstrated that these background magnetic monopole neutrinos can produce the quantum mechanical effect of uncertainty in the position and momentum of the electrons.

Randomly traveling magnetic monopole neutrinos produce an electric field in space that is canceled directionally in space on a macroscopic scale owing to the homogeneous and isotropic distribution of their presence in empty space. However, it does not cancel the strength of the electric field produced by the movement of magnetic monopoles in the atomic and subatomic ranges. This means that the empty space is an electrically charged medium, which is known as an ether in equilibrium that can transmit electromagnetic waves. The electron placed in the space will not stay in the same position, and its exact location will be increasingly uncertain and blurred as time goes by, which is predicted by quantum mechanics. In physics, for a wave to propagate, there must be a medium that carries the wave without exception, although this requirement was waived in the case of electromagnetic waves. According to currently known physics, outer space is considered empty, and there is nothing in it. In addition, although elementary particle physics has found that neutrinos exist in massive numbers in the universe, neutrinos have been considered to have no charges and travel at a speed less than that of light; as such, they are not known to cause any collectively measurable physical effect despite their massive numbers.

On the other hand, the concept of tachyonic magnetic monopole neutrinos relates to the enduring enigma of light waves traveling through the empty (mediumless) space and the uncertainty of the position and momentum of the quantum particle electrons. At the same time, it answers the puzzle of why there are so many inactive and dwindling neutrinos in the universe in such massive numbers. Such a pervading idea of non-interacting chargeless background neutrinos must be incorrect. It is noted that universal intelligence, if it exists, will not waste any small elementary particles inside the universe to ensure that everything runs smoothly. Another enigma addressed by the tachyonic magnetic monopole neutrino hypothesis is the absence of dark energy. We derived the missing dark energy caused by the mutual interaction of the spiraling electric field created by fast-traveling magnetic monopole neutrinos within the previously estimated range of its magnitude.

After further scrutiny, we concluded that it is quite possible that these ubiquitous tachyonic magnetic monopole neutrinos could be the fundamental cause of gravity, which has prompted the investigation of their effect on gravity and writing of this review paper. Newtonian gravity is a mathematical model of how the phenomenon of gravity plays out in celestial mechanics and does not address the core issue of why and how this could be an interesting development in understanding the causes of the phenomenon of gravity in nature. It seems possible to conceptually visualize how gravity may manifest itself from the subatomic-level interaction of tachyonic magnetic monopole neutrinos with virtually impenetrable hadrons, which are essentially quark-gluon plasmas.

2. Hadrons as a Spherical Form of Quark-Gluon Plasma

Since neutrinos are subatomic particles, and protons and neutrons are over 1800 times heavier than electrons, we propose that the main contribution to the gravity

effect is from the interaction between neutrinos and hadrons. From the earlier investigation of the quantum field theoretical investigation of the quark confinement phenomena included in this paper in Section 3, we found that the generalized Yukawa potential derived from the quantum field theoretical calculation of the running coupling constant predicted the asymptotic freedom of the quarks inside the hadron that changes its value depending on the energy scale. At the boundary of the hadrons, the derived QCD potential has a sharply dropping precipitous form, indicating a well-defined boundary of the hadronic particles. The purpose of this study was not to calculate the total energy of the hadron but to show how quarks can be confined. However, as in the case of magnetic monopole neutrinos creating a random electric field in space, fast-moving quarks, which have fractional electric charges inside the hadron, create gluons that have a magnetic field that creates enough energy through mutual interactions to cover the missing mass aside from that of the three quarks. Therefore, hadrons can be considered magnetic glueballs that have no net magnetic monopole, especially in the case of protons, owing to the random orientation of the magnetic field inside. The question is how these magnetic glueballs interact with the traveling tachyonic magnetic monopole background neutrinos in space. The most natural expectation is that the incoming magnetic monopole neutrinos will be scattered in all possible directions when they encounter hadronic quark gluon plasma. In general, when there is no massive object nearby and assuming that the local space time is homogeneous and isotropic without any curvature because of the presence of a massive object, the test object will remain in the same location forever.

However, let us assume that there is a massive gravitating object of mass M at a distance r from the test object. The quark gluon plasma of each hadron inside the massive gravitating object has the property of a randomly fluctuating magnetic field within the shell owing to the fast motion of fractionally charged quarks. On average, there is no definitive direction of the magnetic field. If tachyonic magnetic monopole neutrinos collide with these particles, they bounce off because of the random characteristics of the gluonic magnetic charge distribution. We can expect that the collision of tachyonic magnetic monopole neutrinos with individual hadrons will cause the neutrinos to bounce in every possible direction. In homogeneous and isotropic space, the density of tachyonic magnetic monopole neutrinos is uniform, which means that the impact of the background neutrinos on a hadronic quark gluon plasma will scatter the particles in all directions, which makes the net external force zero, which confirms Newton's first law of motion. However, if there is a massive object of mass M near at distance r from the test object, isotropy of the universal presence of the tachyonic magnetic monopole is disturbed, and the tachyonic magnetic monopole neutrinos will be dispersed at a ratio of $1/(4\pi r^2)$, where r is the distance from the center of mass of the test object to the center of mass of the gravitating object of mass M. (As the distance r increases, the number of neutrinos coming from the direction of the massive gravitating source will increase, and the effect of gravity diminishes). The balance of

the force is disturbed and reduced by the presence of a massive object, and the test object tends to move in the direction of the massive object, which manifests as gravity. In this sense, gravity is a pushing effect of tachyonic magnetic monopole neutrinos from space toward the direction of the other side facing the massive gravitating object that has fewer incoming magnetic monopole neutrinos to compensate for the other pushing force. In fact, Newton, Sage, and Van Flanden proposed that gravity could be a push effect. We can designate a unit of force per impact by a background neutrino and then multiply by the number per second to calculate the total force. A massive particle in space is in a stationary state because this external force is well balanced to cancel each other out in a homogenous isotropic universe. However, the presence of a blockage of the flow of background neutrinos by nearby massive objects causes an imbalance in the force the object experiences otherwise in empty space. Essentially, this is the fundamental cause of gravity that Newton proposed. As expected, this must be the fundamental reason why the inertial mass is the same as the gravitational mass.

Two essential physical discoveries are based on this argument. First, the magnetic monopole charge of a neutron is measured from the magnetic monopole charge of the Earth. Owing to the charge conservation principle, we concluded that neutrinos must have the same magnetic monopole charge because neutrons decay into electrons, protons, and neutrinos. The measured magnetic charge turned out to be extremely small to the degree that it is impossible to measure its strength by tracing the movement of a single neutron, even by using the strongest magnet to cause the deflection of its trajectory. On the other hand, the s-orbital atomic electrons that do not have angular momentum in atomic structures can only be explained by assuming that there is an electric field strong enough to counterbalance the attractive electrostatic force between the proton and the electron in the hydrogen atom. This electric field can be created by fast-moving magnetic monopoles. The idea of quantum mechanics as a type of mechanical force becomes meaningless once it is verified that background tachyonic magnetic monopole neutrinos are the key element responsible for the phenomenon of quantum uncertainty. Within the symmetrized Maxwell equation, a moving magnetic monopole charge must create an electric field along and around its path. Considering the number of neutrinos in the universe and how fast they must travel to compensate for the s orbital electrostatic force in atomic structures, it becomes obvious that the matter objects in the universe are submerged in the sea of tachyonic magnetic monopole neutrinos relying completely on the presence of the tachyonic magnetic monopole neutrinos. As tachyons, neutrinos cannot stop traveling because there is no stationary state for tachyonic magnetic monopole neutrinos. They exist in the realm of opposite symmetry to matter particles in the universe. Their speed, ability to be stationary, and identity to be defined in terms of mass are beyond the range of special relativity, nor do they conform to the same mathematical structure applied to matter particles. In other words, they definitely travel faster than the speed of light and have imaginary numbered masses only because

they do not have to belong to the world only defined by the "real numbered" mass.

The following presentation describes the structure of hadrons made of quark gluon plasma, where the gluons have the property of randomly fluctuating magnetic fields inside the hadrons. The magnetic monopole neutrinos once impacted on the spherical form of the confined fluctuating magnetic field will be dispersed in all directions of the angle omega.

In the following, we discuss how QCD and QED potentials can be found within quantum field theories by using the fundamental mathematical structure of the Yukawa potential and the dimensional regularization method of renormalization in the symmetric form of massless field equations.

3. QCD QED Potentials, Quark Confinement

Abstract

One of the enduring puzzles in high-energy particle physics is why quarks do not exist independently despite their existence inside the hadron, as quarks have never been found in isolation. This problem can be solved by formulating a QCD potential for the entire range of interaction distances of the quarks. This mystery could be related to the fundamental origin of the mass of elementary particles, despite the success of quantum field theories to the highest level of accuracy. The renormalization program is an essential part of the calculation of the scattering amplitudes, where the infinities of the calculated masses of the elementary particles are subtracted for the progressive calculation of higher-order perturbative terms. The mathematical structure of the mass term from quantum field theories expressed in the form of infinities suggests that a finite dynamical mass may exist in the limit when the input mass parameter approaches zero. The Lagrangian recovers symmetry at the same time as the input mass becomes zero, whereas the self-energy diagrams acquire a finite dynamical mass in 4-dimensional space when the dimensional regularization method of renormalization is utilized. We report a new finding that, using the mathematical expression of the self-energy(mass) for photons and gluons calculated from this method, the complex form of the QCD and QED interaction potentials can be obtained by replacing the fixed interaction mediating the particle mass and coupling constants in the Yukawa potential with a scale-dependent running coupling constant and the corresponding dynamical mass. The derived QCD QED potentials accurately predict the behavior of the related elementary particles, as verified by experimental observations.

3.1. Introduction

The standard Glashow-Weinberg-Salem model [1] of electroweak interactions has been highly successful in predicting the interactions of high-energy elementary particles. The discovery [2] of the W and Z gauge bosons, and finally the discovery of the Higgs boson at CERN in 2012 [3], proved that the standard model is a

mathematically correct theory describing the interactions of elementary particles.

However, a consistent interaction potential model has not yet been proposed for QCD and QED. We investigated the structures of the self-energy diagrams of elementary particles to study the relationship between the mass and coupling constant in quantum field theories and applied them to construct the interaction potential model. Using the dimensional regularization method for the renormalization of quantum field theories, a finite indeterminate mathematical form of the dynamical mass of the fields is obtained in the limit of the input mass term in the Lagrangian approaches zero in the dimensional regularization method. In this process, the symmetry of the original Lagrangian is restored, whereas a finite mass appears in the self-energy-loop diagrams. The renormalization group equation [4][1] resolves the problem of arbitrariness in the renormalization prescription. The dynamic mass generation mechanism was presented within the framework of the dimensional regularization method developed by t' Hooft and Veltman [5].

3.2. Dynamical Mass from the Massless Quantum Field Theory

1) $\lambda\varphi^4$ theory

The mathematical structure of the one-loop self-energy diagram in $\lambda\varphi^4$ theory is represented by

$$\text{One loop} = \frac{m_0^2\lambda}{16\pi^2}\left[\frac{1}{n-4}+\frac{1}{2}\psi(2)-\frac{1}{2}\ln\frac{m_o^2}{4\pi\mu^2}+O(n-4)\right], \tag{3-1}$$

where $\psi(2)$ is a constant given in general,

$$\psi(n+1) = 1+\frac{1}{2}+\cdots+\frac{1}{n}-\gamma \quad (\gamma = 0.5772\cdots)$$

and μ is an arbitrary constant with the mass dimensions. Renormalization for a non-zero bare mass m_0 is necessary because the first term is divergent in the $n\to 4$ limit. However, in the zero bare mass limit $m_0\to 0$, the term is not infinite, but becomes undetermined. We introduce a constant C_s, and the one-loop diagram becomes:

$$\begin{aligned}&\lim_{\substack{m_0\to 0\\ n\to 4}}\left[m_0^2\frac{\lambda}{16\pi^2}\left[\frac{1}{n-4}+\frac{1}{2}\psi(2)-\frac{1}{2}\ln\frac{m_o^2}{4\pi\mu^2}+O(n-4)\right]\right]\\ &=\lim_{\substack{m_0\to 0\\ n\to 4}}\frac{\lambda}{16\pi^2}\frac{m_0^2}{n-4}\equiv\frac{\lambda}{16\pi^2}C_s,\end{aligned} \tag{3-2}$$

where

$$C_s = \lim_{\substack{m_0\to 0\\ n\to 4}}\frac{m_0^2}{n-4}$$

As a result of this operation, we have an analytical mass that is not infinity but simply undetermined. Therefore, the massless $\lambda\varphi^4$ scalar field theory begins to

[1]C. Callan, Phys. Rev. D5 (1973) 3202; K. Symanzik, Comm. Math. Phys. 23 (1971) 49; 't Hooft, Nucl. Phys. B61 (1973) 455; S. Weinberg, Phys. Rev. D8 (1973) 3497; S. Coleman, Lecture Erice summer school (1971); K. Wilson, Revs. Modern Phys. 47 (1975) 773; E.C.G. Stueckelberg and A. Peterman, Helv. Phys. Acta 26 (1953) 499; K. Wilson, Phys. Rev. D3 (1971) 1818.

yield a mass from the one-loop self-energy diagram. Recalling that the $\lambda\varphi^4$ massless scalar field theory is the simplest case of supersymmetric theories, it provides us with a clue to a possible mass-generation mechanism for supersymmetric particles.

The fact that the explicit mass parameter in the Lagrangian does not represent the real mass of the field and its sole purpose is to provide a reference from which the real mass can be determined experimentally has already suggested that the mass can be generated by the dynamical interactions of the interacting fields. In the case of the QCD and QED, the self-energy was calculated without explicit mass parameters in the Lagrangian.

2) QED

The self-energy diagram of the electron in the QED without the mass parameter in the Lagrangian is given by

$$\Sigma(p)=\frac{2}{n-4}\frac{e^2}{16\pi^2}P-\frac{e^2}{8\pi^2}\left[\frac{1}{2}P(1+\gamma)+\int_0^1 \mathrm{d}x P(1-x)\ln\frac{p^2x(1-x)}{4\pi\mu^2}\right] \quad (3\text{-}3)$$

where P represents the energy-momentum tensor of the electronic quantum field. Because the self-energy is defined by the energy when the particle is in a resting state, the mass of the electron is given by

$$M_e=\frac{e^2}{8\pi^2}C_e \quad (3\text{-}4)$$

where $C_e=\lim_{n\to 4}\frac{p\to 0}{n-4}\left[\frac{\det P}{n-4}\right]$ and the higher-order small correction terms can be included in the constant factor C_e, without the loss of generality.

The vacuum polarization diagram of the photon is given by

$$\Pi_{\mu\nu}(p)=\frac{e^2}{2\pi^2}\left(P_\mu P_\nu-\delta_{\mu\nu}P^2\right)\left[\frac{1}{3(n-4)}-\frac{1}{6}\gamma-\int_0^1 \mathrm{d}x x(1-x)\ln\frac{p^2x(1-x)}{2\pi\mu^2}\right]+O(n-4) \quad (3\text{-}5)$$

The dynamical mass of the photon is now given by $M_\gamma^2=\frac{e^2}{6\pi^2}C_\gamma$ where the photon mass constant $C_\gamma=\lim_{n\to 4}\frac{p\to 0}{n-4}\left[\frac{\det\left(P_\mu P_\nu-\delta_{\mu\nu}P^2\right)}{n-4}\right]$. Although it is generally known that photons do not carry mass, the gauge invariance of the Lagrangian suggests that they manifest mass in relation to the distance of their interactions with charged particles. In fact, the self-energies of photons and gluons manifest as masses.

3) QCD

Using the same procedure for QCD, the dynamical mass for quarks is given by

$$M_f=C_3\frac{g^2}{8\pi^2}C_f\ C_f=\lim_{n\to 4}\frac{p\to 0}{n-4}\left[\frac{\det P}{n-4}\right] \quad (3\text{-}6)$$

and

$$M_{Y.M}^2=\left(\frac{5}{3}C_1-\frac{4}{3}C_2\right)\frac{g^2}{8\pi^2}C_{Y.M}\ C_{Y.M}=\lim_{n\to 4}\frac{p\to 0}{n-4}\left[\frac{\det\left(P_\mu P_\nu-\delta_{\mu\nu}P^2\right)}{n-4}\right] \quad (3\text{-}7)$$

for the self-energy of the gluon from Yang Mill fields.

3.3. Self-Energy and Coupling Constant in the Quantum Fields

It is well known that the electron mass is related to the electrostatic self-energy in classical electrodynamics, where the radius r_0 of the electron is defined as

$$m_e = \frac{e^2}{r_0}. \tag{3-8}$$

In fact, the relationship between the mass and the corresponding charge of a particle is a universal feature beyond classical electrodynamics. The quantum field theoretical dynamic mass is directly related to the corresponding coupling constants by the following relationships, as shown in the above examples:

$$M_s^2 = \frac{\lambda}{16\pi^2} C_s \; C_s = \lim_{n\to 4} \frac{m_o \to 0}{n-4} \left[\frac{m_o^2}{n-4} \right] \tag{3-9}$$

$$M_e = \frac{e^2}{8\pi^2} C_e \; C_e = \lim_{n\to 4} \frac{p \to 0}{n-4} \left[\frac{\det P}{n-4} \right] \tag{3-10}$$

$$M_\gamma^2 = \frac{e^2}{6\pi^2} C_\gamma \; C_\gamma = \lim_{n\to 4} \frac{p \to 0}{n-4} \left[\frac{\det\left(P_\mu P_\nu - \delta_{\mu\nu} P^2\right)}{n-4} \right] \tag{3-11}$$

$$M_f = C_3 \frac{g^2}{8\pi^2} C_f \; C_f = \lim_{n\to 4} \frac{p \to 0}{n-4} \left[\frac{\det P}{n-4} \right] \tag{3-12}$$

$$M_{Y.M}^2 = \left(\frac{5}{3} C_1 - \frac{4}{3} C_2 \right) \frac{g^2}{8\pi^2} C_{Y.M} \; C_{Y.M} = \lim_{n\to 4} \frac{p \to 0}{n-4} \left[\frac{\det\left(P_\mu P_\nu - \delta_{\mu\nu} P^2\right)}{n-4} \right] \tag{3-13}$$

where C_1, C_2, and C_3 are constants determined by the group structure of the non-Abelian gauge theory, and the sub-indices s, e, γ, f, and $Y.M$ indicate the scalar, electron, photon, fermion, and Yang-Mills fields, respectively. In four-dimensional space, all constants, including the higher-order correction terms for the self-energies, become undetermined in the limit of the momentum, and the input mass becomes zero. These relations between the mass and coupling constant suggest a significant variation in the mass owing to the running coupling constant, which depends on the scale.

3.4. QCD and QED Potentials, Generalized Yukawa Potential

In 1935, Yukawa [6] introduced nuclear potential, which has been proven to be highly successful in addressing many diverse nuclear interactions. The major property of Yukawa's potential is the introduction of the mass of the pion as an interaction-mediating particle, which applies to strong nuclear forces at short distances. The coupling constant and mass of the pion in Yukawa's nuclear potential are independent fixed parameters regardless of the mutual interaction distance.

$$V_{Yukawa}(r) = -g^2 \frac{\mathrm{e}^{-\alpha m r}}{r} \tag{3-14}$$

where g is the coupling constant, m is the mass of the intermediate particle, r is the radial distance between the particles, and α is the scaling constant.

1) QCD

Because we have established the dependence between the scale-dependent coupling constant and the self-energy of the quantum fields, we propose constructing a new generalized Yukawa potential by replacing the fixed mass and coupling constant with those that depend on the running coupling constant (3-2)-(3-7). The generalized Yukawa potential with the variable-scale-dependent running coupling constant and the corresponding self-energy is given by:

$$V_{Yukawa}(r) = -g^2(\mu)\frac{e^{-\alpha m(\mu)r}}{r}, \tag{3-15}$$

where $g^2(\mu)$ is the running coupling constant and $m(\mu)$ is the scale-dependent self-energy (mass) of the interaction-mediating field in the QFT. For example, the photon mass is zero at the macroscopic scale, and the Yukawa potential with zero mass interaction mediating particle takes the form of the Coulomb potential. This property of the Yukawa potential indicates that its fundamental mathematical structure of Yukawa potential is much more general than typically known as the nuclear potential. It has been shown that the coupling constant and mass of the fields depend on the scale of quantum field theory. Therefore, using the property of the generality of the Yukawa potential, it is possible to derive a detailed form of QCD and QED potentials that are effective at the sub-hadronic scale by utilizing the mathematical form of the scale-dependent coupling constant and the mass of the interaction-mediating particles in quantum field theories [7]. The scale-dependent running coupling constant from QCD [4][2] is given by:

$$g^2(\mu) = \frac{g_0^2}{1+\frac{g_0^2}{8\pi^2}\ln\frac{\mu}{\mu_0}} \tag{3-16}$$

which was developed by D. Gross, F. Wilzeck, and H. D. Politzer [8], and using the scale-dependent self-energy of the Yang-Mill field (3-12), the QCD potential is given by

$$V_{qcd}(r) = \frac{g_0^2}{1+\frac{g_0^2}{8\pi^2}\ln\frac{\mu}{\mu_0}}\frac{1}{r}\exp\left(-\left(\frac{\frac{\alpha}{8\pi^2}g_0^2 C_g C_k}{1+\frac{g_0^2}{8\pi^2}\ln\frac{\mu}{\mu_0}}\right)^{\frac{1}{2}} r\right) \tag{3-17}$$

where C_g is the gluon mass constant, which is given by $C_g = 5.8\times10^{-103}g^2$, and C_κ is a group structure constant of an order of magnitude 1 and $g_0 = g(\mu_0)$. However, the potential in the form of (3-17) is impractical because of the parameter μ, which depends on the input momentum scale. To translate parameter μ

[2]E. Stueckelberg and A. Petermann, Helv. Phys. Acta 5 (1953) 499 N. N. Bogoliubov and D. V. Shirkov, Introduction to the theory of Quantized Fields (Interscience, New York, 1959) K. Wilson, Phys. Rev. D3 (1971) 1818 K. Wilson and J. Kogut, Phys. Reports 12 (1974) 75 K. Symanzik, Lett. Nuovo Cimento 6 (1973) 77.

into distance r, we hypothesize that there is a mathematical relationship between μ and r governed by

$$\mu = \lambda \exp\left(\frac{\rho}{r^2}\right), \quad \lambda, \rho > 0 \tag{3-18}$$

where λ and ρ are the adjustable parameters. The relation (3-18) does not violate the quantum mechanical uncertainty because the larger input momentum μ results in a smaller distance r owing to the quantum uncertainty principle:

$$\Delta x \Delta p \geq \hbar/2 \tag{3-19}$$

In fact, the mathematical relation (3-18) is the only possible choice to obtain $1/r$ dependent Coulomb potential at large distances and the QED potential at sub-hadronic distances, which confirms the phenomenological quarkonia spectroscopy results [9].

After the transformation of μ by the relation (3-18), the QCD potential (3-17) is given by

$$V_{qcd}(r) = \frac{1}{\frac{A}{r^2} - B}\frac{1}{r}\exp\left(-\left(\frac{\frac{\alpha}{8\pi^2}C_g C_k}{\frac{A}{r^2} - B}\right)^{\frac{1}{2}} r\right) \tag{3-20}$$

where $A = \frac{g_0^2 \rho}{8\pi^2}$, $B = \frac{\ln\left(\frac{\mu_0}{\lambda}\right)}{8\pi^2} - \frac{1}{g_0^2}$, where the adjustable parameter λ is set to $B > 0$ and C_g is the gluon mass constant, which is given by $C_g = 5.8 \times 10^{-103} g^2$, and C_κ is a group structure constant of the order of magnitude 1.

At $r = r_{cq} = \sqrt{A/B}$, the QCD potential (3-20) becomes zero because of the negative infinite exponential factor, and becomes imaginary as r increases further. To visualize the general structure of the potential, for instance, for $A = B = 1$ and $\frac{\alpha}{8\pi^2} C_\kappa C_g = 0.05$, the QCD potential has the form presented in the diagram in **Figure 1**, which shows the initial confinement and deconfinement by the sharply dropping potential after reaching the maximum and the decay phase as the potential becomes imaginary below the zero level. In quantum mechanics, an imaginary potential is known to violate the conservation of the probability of finding quantum particles. The loss of probability beyond the outer radius of the hadronic boundary is consistent with the absence of fractionally charged isolated particles and with the spontaneous evaporation [10][3] of the black hole at its surface, assuming that the black hole is fundamentally a neutron star with an extremely dense quark-gluon plasma.

For small r and $\alpha = 1$, the QCD potential (3-20) becomes

[3]"Particle creation by black holes" Commun. Math. Phys. 43 (1975) 199 Christian Corda, Classical and Quantum Gravity. 32 (2015) 195007.

$$V_{qcd}(r)=\frac{r}{A}\left(1-\frac{B}{A}r^2+\cdots\right) \tag{3-21}$$

The quark potential (3-20) shown in Figure 1 has the following features.

1) linear potential at small distance r

2) confinement within the hadronic boundary

3) deconfinement beyond the critical distance of the hadronic boundary as the potential drops to zero

4) decay (disappearance) of quark matter as the potential became imaginary as the relative distance increased beyond the zero-potential level.

5) no singularity throughout the relative distances

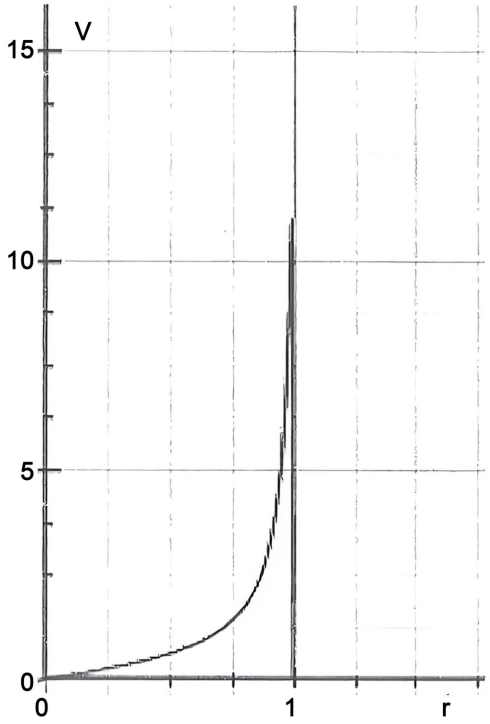

Figure 1. QCD potential diagram.

2) QED

By applying the same mathematical procedure using the running coupling constant for the QED

$$e^2(Q)=\frac{e^2}{1-\frac{e^2}{6\pi^2}\ln\frac{Q}{m_e}}, \tag{3-22}$$

where Q is the input momentum scale given by $Q=\lambda\exp\left(\frac{\rho}{r^2}\right)$ for the transformation into the length parameter r, and λ, ρ are adjustable constants that have the same form (3-18) as in the case of QCD, the QED potential is given by

$$V_{qed}(r)=\frac{-1}{C-\frac{D}{r^2}}\frac{1}{r}\exp\left(-\left(\frac{\frac{\alpha}{6\pi^2}C_\gamma}{C-\frac{D}{r^2}}\right)^{1/2}r\right) \tag{3-23}$$

where $C=\frac{1}{e^2}+\frac{\ln\left(\frac{m_e}{\lambda}\right)}{6\pi^2}$, $D=\frac{e^2\rho}{6\pi^2}$ and C_γ is the photon mass constant (3-10) with an upper limit of the photon rest mass 3×10^{-53} g.

To visualize the detailed structure of the QED potential, for instance, for $C=1$, $D=1$, and $\frac{\alpha}{6\pi^2}C_\gamma=0.01$, the potential is presented in Figure 2, which shows

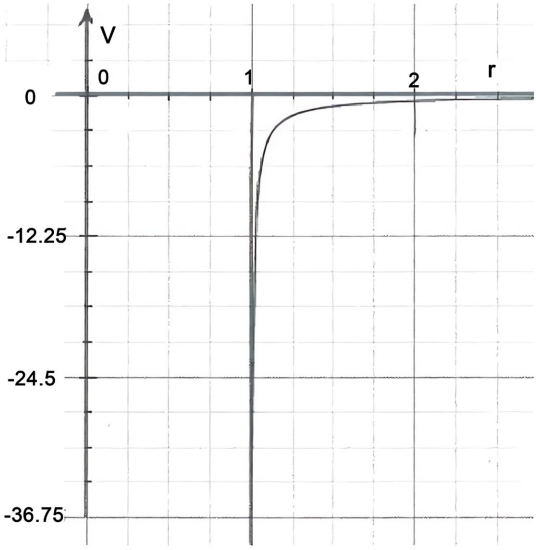

Figure 2. QED potential diagram.

a sharply rising core potential at the contact boundary of the electron and positron at $r=\sqrt{D/C}=1$ as they approach close together. The potential becomes imaginary as both particles come close past the contact distance and reach a level greater than zero. This behavior of the QED potential is consistent with the electron-positron pair annihilation as they approach sufficiently close together. It should be noted that a sharply rising core potential was employed for the calculation of the "Lamb shift" [11] in the form of the $\delta(r)$ function in the phenomenological model. Parameters C and D determine the contact radius of the electron-positron pair and $\frac{\alpha}{6\pi^2}C_\gamma$ determines the depth of the QED potential. By adding the two potentials (3-20) and (3-21) at typical low-energy hadronic bound states, we obtain:

$$V(r)=\frac{-1}{Cr}+\frac{r}{A} \tag{3-24}$$

This result confirms the previously reported non-relativistic phenomenological quark potential, which is in good agreement with the experimental results of heavy

quarkonia spectroscopy [12][4].

The QCD potential (3-20) in **Figure 1** shows a small yet finite probability of finding fractional charges at a critical distance, which supports the results reported by researchers [13][5].

In the case of the QED potential, the interaction of the electron with the antimatter positron is considered key to the loss of the quantum probability of the electron at close distances, which is manifested by the imaginary number of the potential. In the case of QCD, the quark's loss of quantum probability beyond the distance of the hadronic boundary due to the imaginary value of the potential was confirmed by the absence of fractionally charged particles that have never been detected experimentally. The derived QCD potential also confirms the prediction of the spontaneous decay of black holes, which is essentially a large-scale matter state of the quark-gluon plasma.

Conclusion

We presented a uniform mathematical procedure to transform perturbative quantum field theories into an interaction potential model for both QCD and QED by utilizing the running coupling constant derived from the renormalization group equations within the framework of the known Yukawa nuclear potential model and the dynamical mass from quantum field theories. Both the QCD and QED potentials show sharply reversing curvature of the peak potential at the critical distances without the loss of continuity and these two different types of potentials confirm the experimental data at all ranges including the absence of independent isolated quarks and the disappearance of electron and positron in QED by the potentials becoming imaginary beyond the critical distance.

While the presentation is about explaining the phenomenon of quark confinement based on quantum chromodynamics and the electron-positron pair annihilation phenomenon based on QED, the fundamental insight is that protons and neutrons are highly magnetically concentrated quark gluon plasma that bounces off any incoming tachyonic magnetic monopole neutrinos without allowing them to pass through the core of the hadronic structure. This causes the impact mechanism to accelerate the particle in one particular direction if the force is not balanced by the same flux from the opposite direction, which could evolve into the fundamental cause of gravity.

[4]K. J. Miller and M. G. Olsson, Phys. Rev. 25D (1982) 2383; S. Jacobs and M. G. Olsson, Phys. Lett. 133B (1983) 111 E. Eichten, K. Gottfried, T. Kinoshita, K. D. Lane and T. -M. Yan, Phys. Rev. 21D (1980) 203 V. A. Novikov et al., Phys. Reports 41C (1978) 16 A Manohar, H Georgi, Nuclear Physics B. 234 (1984) 189 M Abu-Shady, SY Ezz-Alarab, Few-Body Systems. 3 (2019) 186 R Bonnaz, B Silvestre-Brac, C Gignoux, Eur. Phys. J. A. 13 (2002) 363.

[5]G. S. LaRue, W. M. Fairbank, and J. D. Phillips, Phys. Rev. Lett. 42 (1979) 142; L. J. Schaad and B. A. Hess, Jr., J. P. Wikswo, Jr., W. M. Fairbank, Phys. Rev. 23A (1981) 1600; GL Shaw, R Slansky, Phys. Rev. Lett. 50 (1983) 1959; Yuval Gefen and David J. Thouless. Phys. Rev. B 47, (1993) 10423; Eun-Ah Kim, Michael Lawler, Smitha Vishveshwara, and Eduardo Fradkin Phys. Rev. Lett. 95, (2005) 176402; Eun-Ah Kim, Michael J. Lawler, Smitha Vishveshwara, and Eduardo Fradkin Phys. Rev. B 74 (2006) 155324; XL Qi, Xiao-Liang Qi, Taylor L. Hughes & Shou-Cheng Zhang, Nature Physics 4, (2008) 273; Jie Zhou, Wuhong Zhang, and Lixiang Chen Appl. Phys. Lett. 108 (2016) 111108.

Contrary to the suspicions of some physicists regarding the validity of Quantum Field Theories, Quantum Chromodynamics and Quantum Electrodynamics turned out to be extremely accurate theories of elementary particles, as demonstrated in the above presentation. It was only a matter of finding the correct and theoretically meaningful interaction potential between the electrons, quarks, and gluons arising from the fundamental structure of the theory. The detailed mathematical study of the dimensional regularization method of renormalization in quantum field theories developed by Gerard 't Hooft and Martinus Veltman and the later development of the theory of asymptotic freedom of the running coupling constant in QCD published by David Gross, Frank Wilczek, and David Politzer significantly contributed to the success of this finding.

The discussion so far has mainly focused on the internal quantum field theoretical structure of hadronic particles and how quarks and gluons behave in the form of quark gluon plasma. On the other hand, viewed from outside, where the pervading tachyonic magnetic monopole neutrinos in space are trying to pass through the hadronic structure of the quark gluon plasma, they will experience strong resistance because of the strong potential barrier of the hadronic structure. Fast moving quarks with fractional electric charges inside the hadron create a magnetic field around them and create a randomly fluctuating magnetic glue ball that cannot be passed through by background tachyonic magnetic monopole neutrinos. The reason matter object placed in space maintains its stationary state unless disturbed by external force is because the background distribution of the magnetic monopole flux neutrinos is homogeneous and isotropic which is also dubbed as "flat space time" in general relativity and there is no preferred direction for the object to move forward. However, in the presence of a massive gravitational object nearby, the blockage of the flux of tachyonic magnetic monopole neutrinos by the massive number of hadrons in the object is significant, which affects the locational stability of the nearby mass object. The net effect of the massive object is that the magnetic monopole neutrinos bounce off the massive object and disperse in a random direction but not necessarily in the direction of the nearby matter object, which causes a lack of balance in the position of the test mass nearby. The number of particles that balance the locational stability of the test object is reduced by $1/(4\pi r^2)$, where r is the distance between the massive and test objects. This means that the test object tends to be attracted to the massive object more strongly when the two objects are close together, which is essentially the cause of gravity. In other words, gravity is caused by the imbalance of the neutrino flux toward the test object owing to the blockage of the same flux by the nearby massive object.

We noticed that the concept of magnetic monopole neutrinos fulfills the symmetry of Maxwell's equation between electricity and magnetism simultaneously, and it also explains quantum mechanical uncertainty and the dark energy problem.

The dipole-gravity effect can be explained using the same mechanism. The rotating hemisphere creates an axially asymmetric density distribution of the tachyonic magnetic monopole neutrinos, and the surrounding matter object from the

rotating sphere is pulled in the equatorial direction, where the neutrino density is greatly disturbed, while the axial directional disturbance is minimal in the polar region, which makes the poles an exit door for the incoming matter object pulled into the rotating blackhole from the equatorial side. This implies that dipole gravity is also consistent with the mechanical and conceptual picture of the tachyonic magnetic monopole neutrino model of the Newtonian central gravity phenomenon. The mathematical dipole gravity term was embedded in the linearized theory of general relativity next to Newtonian gravity. The only problem was that the dynamical shift of the center of mass required for this dipole term to be physically meaningful was not immediately obvious because it happens only when a longitudinally asymmetric object such as a hemisphere, cone, or funnel rotates.

The following is a presentation on how the effect of rotation in a longitudinal axially asymmetric object causes a directional gravity effect that is consistent with the observed phenomenon of a flat galactic plane, blackhole jets, Saturn ring, GPB experimental data, and dark matter.

4. Second Order Term in the Linearized General Relativity; Dipole Gravity Originated from Background Magnetic Monopole Neutrinos

Abstract

In addition to the isotropic force from all directions caused by magnetically charged tachyonic neutrinos that cause the gravity effect, the rotational motion creates an additional bounce-off effect in the tangential direction of the rotating quark gluon plasma in every single hadron in the rotating body. The net effect is that the instantaneous density of the background tachyonic magnetic monopole neutrinos becomes uneven in the longitudinal direction of the rotational axis. The wider side of the rotating hemisphere created a lower density than the domed side. This effect creates a condition in which the object tends to move toward lower-density background tachyonic neutrinos.

Blackhole jets, Saturn rings, dark matter, and GPB anomalies are generally considered physically unrelated mysteries with no known common causes that create them. In Newtonian mechanics, the center of mass of an object changes only when an external force is applied to it. However, longitudinally asymmetric and radially circular (LARC) rotating objects such as cones, funnels, and hemispheres have the unique mechanical property of creating a finite dynamic shift of the relativistic center of mass depending on the speed of the rotation. This suggests that the LARC rotating object has complex mechanical properties that do not conform to the conventional Newtonian mechanical principle. In the weak field limit of general relativity, there is a second-order mathematical term that requires a finite shift of the center of mass to establish its physical reality. This term was discarded as physically meaningless because a spherical source does not develop a shift in the center of mass even in rotation owing to mathematical cancelation. It is shown that the relativistic shift of the center of mass from the rotating LARC object is the

cause of the physically meaningful dipole gravity that reduces to the Lense-Thirring force at the center of the rotating spherical shell. However, after careful examination, we found that the signs of Lense-Thirring forces were reversed, and once the signs were corrected, dipole gravity predicted blackhole jets and the flat rotational velocity distribution curve, which is the key evidence of the existence of dark matter. We show that for the rings in Saturn, Jupiter, Neptune, and Uranus, the GPB experimental anomaly is also the result of dipole gravity from the rotating spherical sources.

4.1. Introduction

The center of mass of a physical object plays an important role in Newtonian mechanics as the practical location of an object in space for describing the object's trajectory despite its extended structure. The sphere has been universally chosen as the source of gravity for both Newtonian mechanics and general relativity because of its simplicity in the center of mass, which is located at the center of the coordinate system. Even if the object is not spherical, there is a well-defined unique spatial coordinate that determines exactly where the center of mass is located, and the center of the coordinate system can always be moved to the center of mass of the object without loss of generality. However, in Newtonian mechanics, two steps are required to move the location of the center of mass of an object from one place to another. First, there must be an external force to initiate the movement of the object. Second, there must be another external force to stop the movement after having created the momentum to start the movement according to the first and second laws of Newtonian mechanics [14].

However, we have an unusual case where the LARC rotating object changes its dynamic center of mass without an external force only by spin rotation owing to the special relativistic mass increase effect. Even if initiating the spinning motion is considered an external force, the direction of the shift of the center of mass and the spin-initiating action are perpendicular to each other; thus, the two are not related to the Newtonian mechanical principle of motion. Therefore, LARC rotating objects represent a special mechanical system in which the principle of relativity violates the Newtonian mechanical principle and vice versa. In addition, even though the relativistic mass is not exactly the same as the rest mass of the object, the well-established mass-energy equivalence principle in relativity theory [15] indicates that this is an extraordinary mechanical system that needs to be investigated in detail.

Assuming that the relativistic shift of the center of mass is caused by the reaction from the rest of the universe to equalize the effective location of the rotating hemisphere to the new center of mass, the LARC rotating object must be under the influence of unknown external force initiated by the universe trying to balance the gravitational equilibrium according to Mach's principle [16] which states "local physical laws are determined by the large-scale structure of the universe." This force is continuous because the displacement of the center of mass inside the ro-

tating hemisphere remains the same owing to the conservation of angular momentum. By the time the center of mass of the rest state moved toward the shifted dynamic center of mass, the new dynamic center of mass had already moved further ahead. Despite the constant movement of the rotating hemisphere trying to compensate for the offset center of mass, the shifted center of mass persisted and did not return to zero. Therefore, the most likely scenario is that the rotating hemisphere will continuously accelerate toward the direction of the flat side of the hemisphere where the center of mass is shifted. This means that there is an unknown dynamic gravity field created by the rotating LARC object, which is repulsive on the narrow side and attractive on the wider side. The gravity field lines in the case of the rotating hemisphere come out of the domed side and enter the flat side, similar to magnetic field lines.

The question here is whether this interpretation of the mechanical consequences of the relativistic shift of the center of mass from the LARC object is consistent with general relativity in its mathematical presentation. If so, what would it predict regarding the matter distribution around a rotating blackhole when the full gravitational field produced by the rotational motion of the spherical source in general relativity [17] is considered?

4.2. Relativistic Shift of the Center of Mass and Lense-Thirring Force

According to the traditional presentation of general relativity in the book "Gravitation" in the weak field limit for a slowly rotating spherical source, the dipole gravitational moment appears as a second-order term in the following mathematical expression [18]:

$$\Phi = -\left(\frac{M}{r} + \frac{d_j n^j}{r^2} + \frac{3 f_{jk} n^i n^k}{2r^3} + \cdots \right), \text{ where } n^j = x^j / r \tag{4-1}$$

where M is the total mass energy that is responsible for the active gravitational field and d_j is the dipole moment, which, depending on how one chooses the origin of the coordinates, d_j can be made to zero, and f_{jk} is the reduced quadrupole moment.

On the other hand, from the perspective of the dynamic shift of the center of mass, d_j / M is a vector quantity that defines the direction and physical length of the change in the center of mass due to the rotational motion of the source from the center. $n^j = x^j / r$ is a vector quantity that defines the direction of any point in the coordinate system from the origin. The scalar product of d_j and $n^j = x^j / r$ defines the magnitude of the field strength created by this particular gravitational effect. When the LARC object is placed in an upright position with the wider side up with its stationary center of mass positioned at the origin of the coordinate system, the dynamic shift of the center of mass occurs in the positive z-direction, which simplifies the mathematical analysis of this particular interaction. The importance of this second-order term is that its strength is strong only

next to Newtonian. Moving the origin of the coordinate toward the new dynamical center of mass does not change the dynamics of the system because there is still a separation of the center of mass between the two, that is, static and dynamic.

The fundamental principle of Newtonian mechanics is that the center of mass of an object does not change unless an external force acts on it. By choosing the sphere as the source by default in the weak-field limit, the deciphering process of general relativity automatically excludes the possibility that there may be a case in which the center of mass may change dynamically due to rotational motion.

When the sphere is employed as the source, there is no relativistic shift of the center of mass because of the symmetry of the sphere, even if the sphere rotates along the Z-axis because the dynamic shift of the center of mass from the two oppositely oriented hemispheres cancels each other. The choice of origin of the coordinate system does not affect the dynamics of the system, other than the convenience of the mathematical calculation. Therefore, when only the translation of the coordinate system is considered, there is no displacement of the center of mass that can establish a physically meaningful dipole gravity from the rotating spherical source. Thus, it was concluded from the beginning that the gravitational dipole moment does not exist in the weak-field limit of general relativity.

Later, von Laue [19] presented an argument against the existence of a rigid body in relativity theory. His point of view is consistent with the fact that the finite internal binding force of the material cannot withstand the infinite effective mass when the object rotates quickly, such that the rotational velocity at the outer rim reaches the speed of light. However, apart from the presentation by Weinstein [20] and Phipps [21] that demonstrated that a rigid body can exist in relativity theory, rigidity is considered a relative concept of a solid object because in a room-temperature environment, the rotating body is rigid until the centrifugal force exceeds the particular binding force of the material. Even in the case of ultrafast rotation, as long as the centrifugal force is not strong enough to break the internal binding force of the material regardless of its metallic, molecular, or nuclear origin, the object preserves its form and remains solid. The relativistic mass increase takes effect as soon as the object starts rotating; however, it may be, and so does the shift of the center of mass in the case of rotating LARC objects.

Therefore, it is concluded that a physically meaningful dipole gravitational moment exists regardless of whether a rigid body can exist in relativity theory. Lense-Thirring [22] [23][6] employed a rotating coordinate system in their calculation of the rotation-induced general relativistic dynamic force. Their calculation method technically bypassed the question of rigidity of the source located at the center of the coordinate system.

The center of mass of half of the spherical shell of radius R placed flat side up

[6]22, 29 (1921) Lense, J., & Thirring, H. (1918) Uber den Einfluß der Eigenrotation der Zen, "tralk" orper auf die Bewegung der Planeten und Monde nach der Einsteinschen Gravitationstheorie. Physikalische Zeitschrift, 19, 156-163 (Translation in General Relativity and Gravitation 16 (1984), pp. 727-741).

below the equatorial plane of the spherical coordinate system shifts from $\boldsymbol{r}_0 = \left(0, 0, -\frac{R}{2}\right)$ to $\boldsymbol{r}_c = (0, 0, r_c)$, where r_c is given by:

$$r_c = \frac{-R\dfrac{1-\sqrt{1-\alpha}}{\alpha}}{\sqrt{\dfrac{1}{\alpha}}\sinh^{-1}\sqrt{\dfrac{\alpha}{1-\alpha}}} \tag{4-2}$$

where $\alpha = \dfrac{\omega^2 R^2}{c^2}$.

When the speed of the rotational frequency is slow $\omega R \ll c$ in the non-relativistic regime, the shift in the center of mass is given by

$$\delta r_c = \frac{\omega^2 R^3}{24c^2} \tag{4-3}$$

The gravity potential, including dipole gravity from the slowly rotating hemispherical shell placed in a bowl configuration in a spherical coordinate system, is given by

$$\Phi = -\frac{M}{r} - \frac{d_z}{r^2}\cos\theta + O\left(\frac{1}{r^3}\right) \tag{4-4}$$

where

$$d_z = M\delta r_c = M\frac{\omega^2 R^3}{24c^2} \tag{4-5}$$

The origin of the coordinate system is located at the center of mass of the hemisphere, which is in the middle between the pole and the center of the full sphere.

The full gravity potential of the rotating spherical shell, which consists of two oppositely oriented rotating hemispheres, is given by.

$$\Phi = -\frac{M}{r} - \frac{d_z/2}{\left|-(R/2)\hat{z} - \overline{r}\right|^2}\cos\theta' + \frac{d_z/2}{\left|(R/2)\hat{z} - \overline{r}\right|^2}\cos\theta'' + O\left(\frac{1}{r^3}\right) \tag{4-6}$$

where

$$\theta' = \tan^{-1}\left(\frac{r\sin\theta}{r\cos\theta + R/2}\right)$$

$$\theta'' = \tan^{-1}\left(\frac{r\sin\theta}{r\cos\theta - R/2}\right)$$

There is non-zero dipole gravity field from the rotating sphere despite the opposite orientation of the two hemispheres due to the fact that the centers of mass of the two hemispheres are separated by the distance *R*. There are two repulsive dipole gravity poles, one in the North and the other at South, and two attractive poles near the center in the rotating sphere, independent of Newtonian gravity.

At the limit of the low speed of rotation, the dipole gravity force from the rotating spherical shell in the Cartesian coordinate system is given by in the form of the equation of motion:

$$\ddot{x} = -\frac{2M}{R}\omega^2 x$$
$$\ddot{y} = -\frac{2M}{R}\omega^2 y \tag{4-7}$$
$$\ddot{z} = \frac{4M}{R}\omega^2 z$$

The Lense–Thirring force from the slowly rotating spherical shell is given by:

$$\ddot{x} = \frac{M}{3R}\left(\frac{4}{5}\omega^2 x - 8\omega\upsilon_y\right)$$
$$\ddot{y} = \frac{M}{3R}\left(\frac{4}{5}\omega^2 y + 8\omega\upsilon_x\right) \tag{4-8}$$
$$\ddot{z} = -\frac{8M}{15R}\omega^2 z$$

which includes the velocity dependent Coriolis force.

In addition to the tangential velocity-dependent Coriolis force, the dipole gravity force (4-7) from the rotating spherical shell is identical to the Lense-Thirring force (4-8) within the multiplication factor, $-\frac{2}{15}$. The signs of the Lense-Thirring force (4-8) indicate that the radial component of the force is repulsive and the axial directional force is attractive.

The repulsive radial component of the Lense-Thirring force is consistent with the interpretation of the centrifugal force, originally suggested by Einstein. The problem with this sign designation is that there is no physical interpretation of the attractive Z directional force, which is left unassigned once the repulsive radial components of the force are interpreted as the centrifugal force because the axial and radial components of the Lense-Thirring forces always appear in pairs because they originate from the same mathematical representation.

4.3. Sign Controversy in Lense-Thirring Force

Cohen and Sarill [24] discussed the centrifugal force component of the Lense-Thirring force earlier and suggested that it must originate from the quadrupole effect. Bass and Pirani [25] presented a similar argument regarding the origin of the radial component of the Lense-Thirring force as a result of the latitude angular dependency of the velocity of the rotating spherical shell. There were questions regarding the validity of the interpretation of the radial component of the Lense-Thirring force as centrifugal force.

Because Lense-Thirring forces are identified as having originated from the dipole gravity of the second-order term in linearized general relativity, as can be seen from the identical mathematical structure except for the constant multiplication factor, there were no reasons to question the validity of the original signs of Lense-Thirring forces, and it was presented that dipole gravity produced Lense-Thirring force including the signs. However, it became obvious that the adopted signs of the Lense-Thirring force originating from Mach's principle for dipole gravity are not compatible with other cosmological problems, except for the ob-

served anomalous red shift that does not require the accurate designation of the direction of the force from dipole gravity.

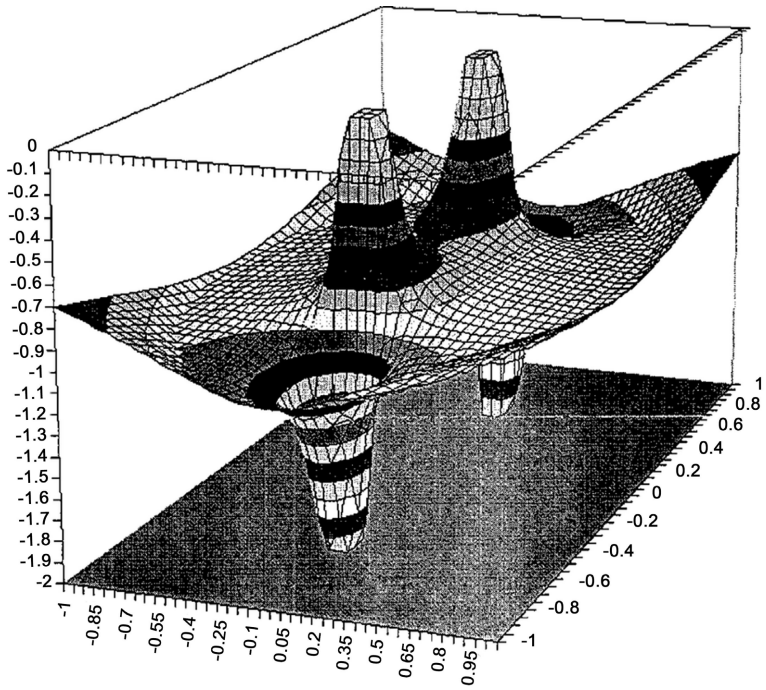

Figure 3. Dipole gravity potential from rotating sphere with reversed polarity: four poles are aligned along the rotation axis with the saddle point located at the center.

After the publication of the first paper, we found that dipole gravity cannot explain other cosmological problems such as jets and dark matter problems. As a new force of gravity, one would expect it to explain certain other cosmological problems. To elucidate the problem in detail, once the signs of the Lense-Thirring force are adopted for dipole gravity, the gravity potential (4-6) is represented by the potential diagram shown in **Figure 3**, where two sets of dipole gravity potentials are aligned face to face along the Z-axis. As Cohen and Sarill suggested earlier, the Lense-Thirring force came out of the quadrupole field configuration along the axis of the rotating spherical shell, as shown in **Figure 3** and **Figure 4**.

Incidentally, there were no additional studies on the Lense-Thirring force in the literature after Cohen, Sarill, and Vishveshwara [26] questioned the centrifugal force origin of the radial component of the Lense-Thirring force and claimed that it must originate from the quadrupole effect.

The saddle potential at the center of **Figure 4** represents the Lense-Thirring force and its sign, where the potential indicates a downward (repulsive) equatorial force and upward (attractive) longitudinal directional force.

The integral equation set forth by Lense-Thirring using the rotating coordinate model to find the gravity field created by the rotating spherical shell cannot be solved, except near the center of the sphere, owing to the mathematical divergence

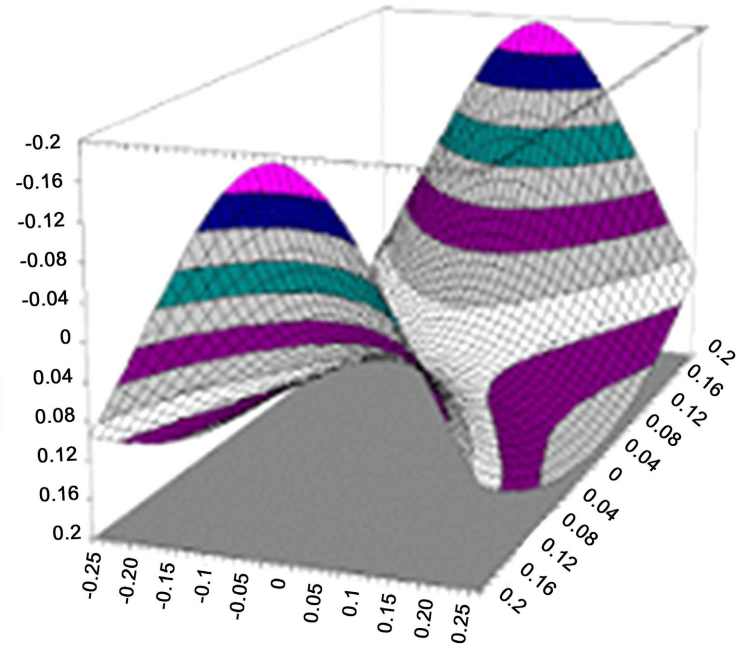

Figure 4. Magnified saddle potential of reversed polarity from rotating source representing Lense-Thirring force.

problem. This drawback resulted in the ambiguity of the detailed structure of the rotation-induced gravity field far from the center, inside and outside of the rotating spherical shell, and especially the question of where this force originated. As such, the true cause of the Lense-Thirring force has remained a mystery since their study was first published in 1918. Bass and Pirani discussed the possible origin of the Lense-Thirring force from the latitude-dependent velocity distribution of a rotating sphere. Pietronero and Cohen, Sarill, and Vishveshwara proposed that the origin of the centrifugal force in the Lense-Thirring force must be the quadrupole gravity effect. In fact, the two oppositely superposed dipole gravitational fields display a single quadrupole field represented by four poles inside the rotating sphere, as shown in **Figure 3**. However, the dipole gravity potential with the adopted signs from the Lense-Thirring force shown in **Figure 3** is strongly attractive at the poles and does not have an application for known cosmological problems, especially for jets from black holes.

On the other hand, viewed from the fundamental principle of mechanics, the fact that the dynamic center of mass shifts toward the flat side of the rotating hemisphere indicates that there is an unbiased effort by the rest of the universe to balance the equilibrium of the center of gravity of the rotating hemisphere toward the direction of the flat side. This point of view is consistent with Mach's principle, which states that "local physical laws are determined by the large-scale structure of the universe." This also means that the force experienced by a test object placed at the dome side of the rotating hemisphere is repulsive and attractive on the flat side, originating from the shift of the center of mass due to the velocity-dependent relativistic mass increase effect.

Another way to view the problem is by questioning the change in the force of gravity that a test body experiences outside the spherical shell in the horizontal plane when the sphere starts to rotate. The first-order change in the force will be toward the center of the sphere because the rotational kinetic energy increases the total mass energy of the spherical shell. Therefore, the rotation-induced gravity force on the horizontal plane from the outside must be attractive toward the center. On the other hand, the constant change in the linear momentum of the mass attached at the end of the string in circular motion creates a centrifugal force, which is an outgoing force that does not have a latitudinal angular dependency based on the analysis of the rotating spherical shell presented by Cohen *et al.* This indicates that the centrifugal force has no relation to the physical origin of the Lense-Thirring force.

Therefore, we concluded that the signs of the Lense-Thirring force were reversed, and once dipole gravity has its correct signs (4-6) (4-7) recovered, we have the full double dipole gravity fields from the rotating sphere 180˚ turned from the one shown in Figure 3.

The two repulsive poles are located at the north and south pole of the rotating sphere and the two attractive ones at the center of the horizontal plane that pull back the matter particles toward the center and then repel particles from the poles because the dipole gravity field lines from the two rotating hemispheres have closed loops, such as magnetic field lines. The equatorial plane of the rotating galaxy becomes a stable resting place where matter particles that come out of both poles have time to merge together and start nuclear synthesis to generate heat, light, and form planetary systems. This was caused by the angular component of dipole gravity from the two rotating hemispheres canceled at the equatorial plane and formed a narrow potential dip around the circumference.

The repulsive dipole gravity at the poles of the rotating source also indicates that the galaxy with a rotating blackhole at the center is not planar in shape, but that the full space is filled with flying matter particles of limited sizes. These flying matter particles are not visible to the telescope because they do not have enough mass to start nuclear fusion to produce light.

4.4. Matter Distribution Due to the Jets, Accretion Disc, Flat Rotational Velocity Distribution Curve and Dark Matter Problem

The Newtonian central gravity potential created by the matter distribution $\rho(r)$ caused by the ejected matter particles from both poles of the rotating black hole at the center of the rotational galaxy is given by in the differential form:

$$\mathrm{d}V(r)=\frac{\rho(r)}{r}4\pi r^2\mathrm{d}r \tag{4-9}$$

where $\rho(r)$ is the matter density distribution along the radius of the galaxy from the center. The trajectories of these particles follow dipole gravity field lines, which are similar to magnetic flux lines. The matter flux coming out of both poles

of the black hole forms a large loop in space until it reaches the horizontal galactic plane. The range of the matter flux is not infinite, but it has a certain range depending on the initial kinetic energy they carry off the rotating black hole at the center of the galaxy.

In the range from the radius of the blackhole to the far outreach of the galaxy, the matter flux distribution will be close to originating from narrowly positioned two-point sources moving outward in all spherical directions. Therefore, the matter flux density multiplied by the spherical area $\rho(r)4\pi r^2$ must be constant.

$$\rho(r)4\pi r^2 = const \tag{4-10}$$

The gravitational potential created by this matter distribution is given by

$$V(r) = \int \frac{\rho(r)}{r} 4\pi r^2 \mathrm{d}r = \int \frac{const}{r} \mathrm{d}r = const \times \ln(r) \tag{11}$$

The logarithmic gravity potential is known to produce a flat rotational velocity distribution curve [27], which is observed in rotating galaxies.

The strong radial dipole gravity dominates the gravitational force at a short distance r from the center but outside the black hole, which is given by

$$F_{dipoleradial} = \frac{-3M\delta r_c R}{2r^4} \tag{4-12}$$

in the range of $r > R$, where M is the mass, R is the radius of the rotating source, and δr_c is the relativistic shift of the center of mass from half of the sphere. The radial component of the dipole gravity force depends on $\frac{1}{r^4}$ instead of $\frac{1}{r^3}$ because of the contribution of the latitude-angular-dependent component of dipole gravity. This explains the sharply rising slope of the rotational velocity distribution curve near the galactic center. The Coriolis force provides a velocity-dependent force in the tangential direction, which contributes to the strong spiraling effect of the accretion disk near the galactic center.

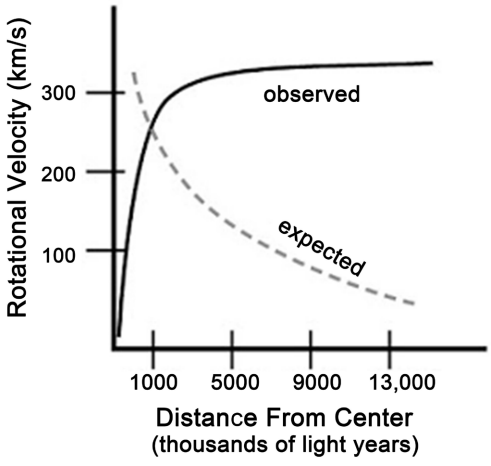

Figure 5. Flat rotational velocity distribution curve
Courtesy of Dr. Greg Bothun.

The fundamental mystery of the dark matter problem was "what causes the flat rotational velocity distribution curves observed from the rotating galaxies?" and "where are all the matter particles that contribute to this effect?" The matter distributed along the equatorial plane follows the same pattern of decreasing mass density as the distance from the center increases, which follows the same logarithmic potential that results in the flat rotational velocity distribution curve shown in Figure 5.

This analysis indicates that the missing dark matter is scattered all over the galaxy in the form of matter particle flux originating from the center of the black hole. They are not visible because they do not emit light owing to their limited mass, which is not large enough to initiate nuclear fusion. The range of the flat rotational velocity distribution curve does not stretch to infinity, as confirmed by researchers in the field. This is because the flying matter has limited kinetic energy in such a way that its trajectory does not stretch to infinity and it does not end abruptly at the edge of the galaxy because of the thermodynamic property of the initial kinetic energy carried by the matter particles ejected from the black hole.

4.5. Jets, Heavy Atomic Element Formation and Wobbling Blackhole

The long stretch of light display observed from the rotating galaxy is attributed to the collision between the outgoing and incoming matter objects toward the center along the rotation axis, which causes a massive firework. This occurred because the initial kinetic energy given to the matter ejected from the center of the black hole was limited, as shown in the dipole gravity potential well between R/2 and R along the rotation axis.

The dipole gravity potential diagram in Figure 6 shows a side view along the Z axis of the rotating sphere. The matter objects in the galactic plane are pulled into the center through the accretion disk of the horizontal plane, which is vertical to the Z-direction, as shown in Figure 6. The height of the wall of the dipole gravity potential well increased as the speed of rotation of the black hole increased. The enormous compression of matter objects in this process creates heavy atomic elements that are readily distributed throughout the galaxy.

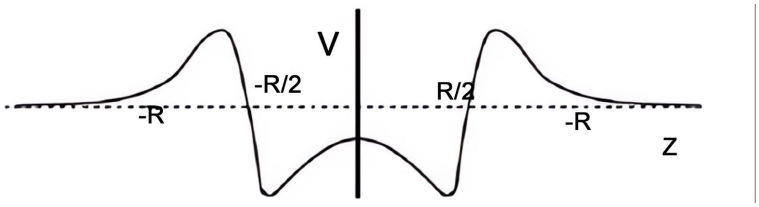

Figure 6. Z directional component of dipole gravity potential from the rotating spherical source. The potential shows the matter particles are repelled toward both the N and S poles of the rotating source.

Once the dipole gravity potential well is filled with matter particles, there are two points of the peak potential, as shown in Figure 6, where the attractive New-

tonian gravity cannot fully contain the molten matter particles, which is the point where the matter objects start spilling. The spilt over molten matter objects owing to high compression is pushed down the steep potential well along the two opposite poles of the black hole. The sudden release of pressure causes molten matter objects to change their phase into fragmented particle states of matter. This mechanism shows how matter objects are capable of exiting the rotating blackhole at the galactic center based on the principle of the dynamic gravitational dipole moment.

The matter objects went out straight up along the Z axis and returned once the initial kinetic energy obtained from the repulsive dipole gravity reached the level of the central gravity potential at a far distance r because the strength of the dipole gravity fell off rapidly as the distance increased. The collision between incoming and outgoing matter objects along the rotation axis of the black hole is inevitable, and they produce large amounts of light, which are observed as blackhole jets. The ejected matter particles that did not go out straight line followed the dipole gravity field lines in the galactic space, drawing the dipole field curve until they arrived at the galactic plane where they met other particles ejected from the opposite pole of the black hole. After a certain period of back-and-forth oscillation centered on the horizontal galactic plane and losing kinetic energy, the matter particles settle down, and the clusters form individual planetary systems.

However, if the axis of the rotating blackhole wobbles because of the additional off the axis angular momentum, there is a chance that visible jets may not be formed because the incoming and outgoing matter objects can avoid collision along the rotation axis. Even if this is the case, the rotating galaxy with the wobbling axis still ejects matter particles, and they manifest the same dark matter problem because the absence of visible jets only means that the longitudinal polar orbit is not stationary owing to the wobbling effect.

4.6. Galactic Plane, Rings in Saturn, Jupiter and Uranus

Aside from the blackhole, fast-rotating planets also create a dipole gravity field that is not strong enough to produce jets, but has an appreciable strength of the angular component of the dipole gravity potential, which creates a dip in the horizontal plane of the rotation that catches the flyby satellite matter objects and harbors them for long periods of time, which are observed as rings. Rings were observed in Saturn, Jupiter, Uranus, and Neptune in our solar system. The two angular components of the oppositely oriented dipole gravity fields cancel each other in the horizontal plane of the rotating planet, where matter objects, including ice particles, tend to settle down. The formation of the hexagonal pattern at the poles of Saturn indicates that while the planet does not have jets, the repulsive dipole gravity effect is not entirely negligible at the poles relative to the Newtonian central gravity, which allows matter objects on the ground of the poles to slide around the fluid influenced by the centrifugal force to form a specific geometrical pattern.

4.7. GPB Anomaly and Figure 8 Lissajous Curve

The GPB gyros [28][7] are oriented to point stars located far from Earth. The satellite circled around the polar orbit from the North to South Pole of Earth. They reported a reversal of the direction of the precession of the gyros when the satellite passed the equatorial plane. As presented above, half of the rotating Earth constitutes a gravitational dipole moment; therefore, there are two dipole moments superposed in opposite directions on the way of the satellite from the North to South Pole.

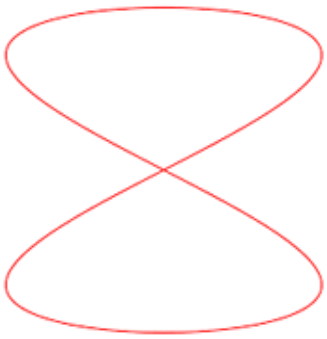

Figure 7. Figure 8 (2 × 1) Lissajous curve.

Because the axis of the gyro points to the remote star, the magnitude of the force causing the precession changes every 1/4th (90˚) revolution of the craft, and the latitude angular component of the dipole gravity force of the Earth changes its direction after the craft crosses over the equator for the next 1/4th (90˚) revolution up to the south pole.

Therefore, there is a 2:1 ratio of the period of the force influencing the precession of the gyro, that is, the direction of the force on the gyro changes along the latitude angle (from zero to 180˚), as shown in **Figure 7**. On the other hand, the frame dragging force along the direction of the motion of the Earth's surface does not change its direction in half of the revolution of the spacecraft around the path from the North to the South Pole. In such cases, the precession of the gyro is circular (1 × 1 Lissajous Curve).

The Lissajous curve cannot be closed unless the ratio $a \times b$ is an integer multiple of [29]. The observed closed 2 × 1 Lissajous curve is unique, and it is unlikely that this type of precession is caused by the random electrostatic patch effect [30]. Consistent closed-looped Lissajous curves from the three separate gyros, as shown in [31], indicate that there are no significant systematic errors due to the electrostatic patch effect. The point of curvature change from right-to left-handed rotation in the Lissajous curve coincides with the point where the latitude-angular-dependent dipole gravity force reverses its direction at the horizontal plane.

[7]Wechsler, Risa; Tinker, Jeremy (September 2018) "The Connection between Galaxies and their Dark Matter Halos" Annual Review of Astronomy and Astrophysics.56: 435-487.arXiv:1804.03097. Bibcode:2018ARA&A. 56. 435W. doi:10. 1146/annurev-astro-081817-051756. S2CID119072496.

According to the report, the detected precession effect from the gyros was much larger than originally expected, according to the prediction of the gravitomagnetic frame dragging effect. The three videos of the gyro motion published by NASA [32] indicate that the original rotational speed of the gyro was reduced in the second and third experimental cases, as shown in the videos, because the Lissajous curve of the first one was very large and almost out of scale. The consistent **Figure 8** of the gyro's movement in all three cases indicates that there was not much random electrostatic patch effect; however, the experiment was a clear manifestation of the oppositely superposed second-order effect in the linearized theory of general relativity originating from the rotating Earth.

4.8. Conclusion

We presented a case in which the relativistic shift of the center of mass from the rotating LARC object creates a dipole gravity field in the weak field limit of general relativity based on the mathematical presentation associated with the Lense-Thirring force. The typical forms of the source that creates a single dipole gravity effect are hemispheres, cones, and funnels, which may be called monotonic LARC objects because of the uniform directional slope, unlike a sphere that has two oppositely oriented slopes in the longitudinal direction. As such, a rotating uniform cylinder does not create a dipole gravity field, owing to the absence of a longitudinal slope. The strong central gravity tends to force stellar or planetary objects to become spherical, which is essentially the cause of the opposite double dipole gravity field from the rotating spherical source. If any single LARC astronomical object in the universe rotates quickly, it will cause an effect reminiscent of the anomalous red shift observed in astronomy. The dipole gravity force lines resemble the magnetic field lines, and this force is the cause of the blackhole jets and dark matter problem in cosmology when two oppositely oriented dipoles are in action at the center of the galaxy. The thin rings observed around the fast-rotating planets Saturn, Jupiter, Uranus, and Neptune in the solar system are due to the two oppositely positioned latitude angular-dependent dipole gravity fields from the spherical source that cancel the horizontal plane, which creates a narrow potential dip around the equatorial plane of the fast-rotating planets.

A rotating hemisphere is a typical example of a longitudinal axially asymmetric object that creates an attractive dipole gravity force from the flat side of the hemisphere. This is a new force of gravity that is not apparent in the linearized theory of general relativity. The vague hint was there asking for a meaning of the strange shift of the center of mass that does not exist in Newtonian mechanics. Naturally, it is discarded as a meaningless mathematical term in many mathematical formulations in physics. While contemplating for a long time that this term must have some kind of meaning, it was dawned onto the author in 1995 that a rotating hemisphere, cone, or funnel can develop a special relativistic shift of the center of mass, and a rotating sphere will cancel this shift of the center of mass in the first order. Later, it was found that this term was directly related to the Lense-Thirring force,

which was explained in detail above. In fact, Figure 6 explains how massive nuclear elements can be formed in the universe in the process of enormous compression at the core and ejection of the matter particles along the z axis of the rotating black hole at the center of the rotating galaxies, as another example not mentioned in the above text.

The following presentation presents the details of the experimental measurement of the single magnetic monopole charge of neutrons stemming from the massive number of neutrons on Earth and consequently that of neutrons due to the universal charge conservation principle. The sheer number of neutrinos in the universe makes it impossible to ignore their effect on the motion of matter objects once they are determined to have magnetic monopole charges and tachyonic properties in nature.

5. Measurement of Magnetic Monopole Charge of the Neutrinos; Aether, Dark Energy and Quantum Mechanical Uncertainty

Abstract

Charge conservation in elementary particle physics theory is one of the best-established principles in physics. As such, if there are magnetic monopoles in the universe, the magnetic charge will most likely be a conserved quantity such as electric charges. If neutrinos are magnetic monopoles, as physicists have reported, the Earth should show signs of having a magnetic monopole charge on a macroscopic scale because neutrons must also have a magnetic monopole charge if the general charge conservation principle is valid. To test this hypothesis, experiments were performed to detect the collective effect of the magnetic monopole charge of neutrons on Earth's equator using two balanced high-strength neodymium rod magnets. We were able to identify the non-zero magnetic monopole charge of individual neutrons from the experiments. The presence of individual magnetic monopole charges in the universe prompted the proposition of a new symmetric form of Maxwell's equation. Based on the theoretical investigation of Maxwell's equations, we conclude that magnetic monopole neutrinos are the cause of quantum mechanical uncertainty, dark energy, and the medium for electromagnetic wave propagation in space.

5.1. Introduction

In 1931, Dirac theorized that for an electric charge to be quantized, a magnetic monopole must exist [33]. In 1974, Polyakov [34] and t' Hooft [35] discovered that the existence of monopoles follows from general ideas about the unification of fundamental interactions.

Other pioneers in the field, Alan Chodos [36], E. Recami [37][8], O.M.P. Bilaniuk, V.K. Deshpande [38], O.M.P. Bilaniuk, and E.C.G. Sudarshan [39] discussed the

[8]Report. November 1973 Recami, E. "Classical Tachyons and Possible Applications: A Review" Riv. Nuovo Cim. **9**, 1-178, 1996.

possible existence of tachyons. Some GUTs [40], such as–the Patient Salam model [41] and superstring theory [42], predicted the existence of magnetic monopoles as well. Ricami and Steyaert [43] discussed the possibility of neutrinos being tachyonic-magnetic monopoles.

Recently, a joint experimental team from the UK, South Africa, Spain, France, and Brazil [44] reported that the lightest neutrinos have an upper bound mass of 0.086 eV with a 95% confidence level. However, stationary neutrinos have not been detected, either directly or indirectly, which is necessary to prove that neutrinos are de facto ordinary matter particles. In addition, there is no evidence that right-handed neutrinos are most likely to be observed if neutrinos can be stationary. Neutrinos have the unusual property of mass oscillation between flavors, which has not been observed in electron families. Therefore, the question of whether neutrinos are tachyons, whether there are magnetic monopoles in the universe, and/or whether neutrinos are both tachyons and magnetic monopoles remains one of the great mysteries of the universe.

In conventional nuclear beta decay processes, a neutron decays into a proton, electron, and antineutrino, as follows:

$$ {}^{1}_{0}n \rightarrow {}^{1}_{1}p + {}^{0}_{-1}e + {}^{0}_{0}\overline{\nu}_{e} \tag{5-1} $$

The electric charge and baryon number are conserved in the process, whereas the neutrino carries leftover energy and momentum. In this form of weak decay, the neutrino is an inactive subatomic particle because it does not have any type of charge, and once it loses its energy, there is no interaction between the neutrino and other particles, which is unusual from a utilitarian philosophical perspective, especially considering their massive presence in the universe.

In this report, we present new experimental evidence that neutrinos are light magnetic monopoles by measuring the Earth's magnetic monopole charge originating from a massive number of neutrons based on the general charge conservation principle in particle physics.

5.2. Experimental Principle

5.2.1. Test Bar Magnets

There are a substantial number of neutrons in atomic elements on Earth in their composite nuclear structures. In essence, the task of measuring the magnetic monopole charge of a neutrino is to measure the Earth's magnetic monopole charge of neutrons based on the assumption that the magnetic charge is conserved.

If a well-balanced long cylindrical high-strength test magnet with a pivot at its midpoint is placed in the horizontal position near the equatorial surface of the Earth, the assembly will tilt toward one side or the other, depending on the polarity and strength of the Earth's magnetic monopole charge.

The measurements were conducted separately using two long permanent test bar magnets composed of an even number of stacked cylindrical disc neodymium magnets. The two bar magnets have different magnetic strengths, diameters, and lengths of their long cylindrical forms. The center of the bar magnet was placed

on the pivot of a tightened string made of non-magnetic material with negligible thickness to ensure minimum torque resistance on the test rod magnet to minimize obscuring the experimental data. Any minute tilting force on the sensor magnets is measured in the horizontal position using a precision microscale to reflect the collective magnetic monopole charge of neutrons on Earth.

5.2.2. Optimum Geographical Location for the Experiment

The most critical task in the experiment is to separate the effect of the Earth's dipole geomagnetic field on the balance of the detector magnet for accurate measurement of the magnetic monopole charge of the Earth. Hence, it is critical to choose the right location on the surface of the Earth to minimize the geomagnetic effect from entering the measurement. As shown in **Figure 1** and **Figure 2**, a location near the equator is necessary to avoid any vertical component of the dipole geomagnetic field entering the data in the first order. In addition, if Earth had a perfectly even density and uniform surface, any location near the equator would be acceptable in the second order. However, the presence of deep-sea ocean, which is filled with water with a very low density of neutrons, high mountains with a large concentration of neutrons above the ground, and volcanoes that have an irregular density of underground matter can cause unnecessary errors in the measurement of the Earth's magnetic monopole field. Therefore, we decided to choose Cuenca as the location to perform the experiment because Quito is too close to the two volcanoes in Pichincha 24 km in the north and Cotopaxi 50 km in the south. Cuenca is located 450 km south of Cotopaxi and 104 km east of the Pacific Ocean, which is considered reasonably far from the geographical aberration. Although the satellite measurement of the Earth's magnetic field has consistently remained minimal in the region of Peru in South America instead of the equatorial region in Ecuador, the accurate angular orientation of the satellite-measured geomagnetic field is not known or specified. Therefore, the vertical component of the measured geomagnetic field strength is not reflected separately in the satellite data. In addition, the quadrupole geomagnetic field strength is generally known to be less than 10 percent of the dipole magnetic field, and as such, in combination with a possible geographical misplacement, the systematic error in the measurement is less than ±10%. It is noted that satellite measurements of the earth's magnetic field have not found a particular region on Earth where the measured geomagnetic field is zero.

5.2.3. Precision Balancing of the Test Bar Magnets

The next critical factor is to balance the weight of each half of the bar magnet on both sides of the pivot because unless the test magnets are precisely balanced, including the magnetic field strength, weights, and length, the measurement of the earth's magnetic monopole strength would be inaccurate. The problem of balancing the weight of the bar magnet is that in addition to the actual weight due to the mass, there are magnetic forces affecting the measurement. This is achieved in the first order by choosing an identical number of uniform-sized disk magnets on

both sides and second by selecting four disk magnets with a magnetic strength of ±1% measured by a precision magnetometer and placing them at the end of each of the bar magnets because there are measurable differences within ±5% in the field strength among the disk magnets. Because the thickness and radius of each disk magnet are factory set, the accuracy of the length and weight of both sides of the bar magnets is extremely high, with a difference of less than ±1%. The third step calibration is performed by measuring the weight of each half of the bar magnet by placing each separately in a vertical position on the micro scale with the N pole side down and by compensating for any minute difference in weight by adding ten milligram range of weight in the middle of the lower weight side of the bar magnet. After the adjustment, both sides of the bar magnet turned out to have a mass, length, and magnetic field strength at the end within an error of ±5%.

5.3. Measurement and Analysis of Experimental Data

5.3.1. Details of the Experiment

We chose a location (2.899350˚S, 78.989264˚W) in Cuenca Ecuador, a city close to the equator with a high plateau, equipped with two sets of long neodymium cylindrical bar magnets, a precision magnetometer (WT10A), and a precision digital microscale (AMOTGR 2001). One of the assembled neodymium magnets had a length of 19 cm and a diameter of 10 mm, where both sides had magnetic fields of the same magnitude as measured by the precision magnetometer, and the other neodymium dipole magnet had a length of 16.6 cm and a diameter of 12 mm. The earth, as a monopole magnet, is expected to exert a magnetic force on these test magnets by pulling down on one side and pushing up the other when the balanced dipole magnet is placed horizontally resting on a tightened string of negligible thickness (Figure 8).

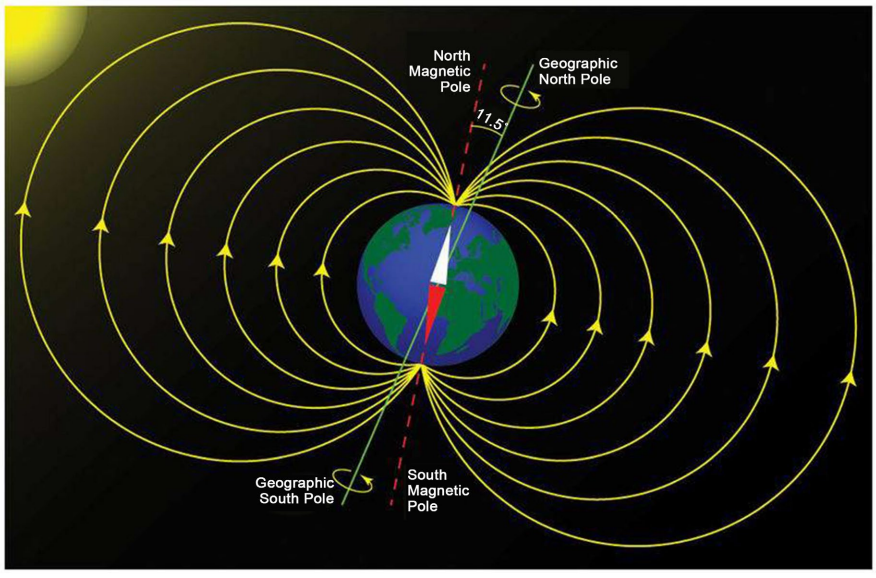

Figure 8. Curved Earth's geomagnetic field lines.

If consistent measurable tilting occurs on the two different-precision balanced magnetic monopole sensors near the equator, it indicates that the Earth has a magnetic monopole charge stemming from the accumulative magnetic monopole effect of its neutrons.

A close-up depiction of geomagnetic field lines is shown in Figure 9, which shows that in the northern and southern hemispheres, there is a strong vertical component of the geomagnetic field because the geomagnetic field lines converge toward the poles and are no longer horizontal to the surface of the Earth, except near the equator. This vertical component of the geomagnetic field cannot be distinguished from the central monopole magnetic field originating from the neutrons of the Earth in the measurement; therefore, we chose the equatorial region of the Earth to perform the experiment.

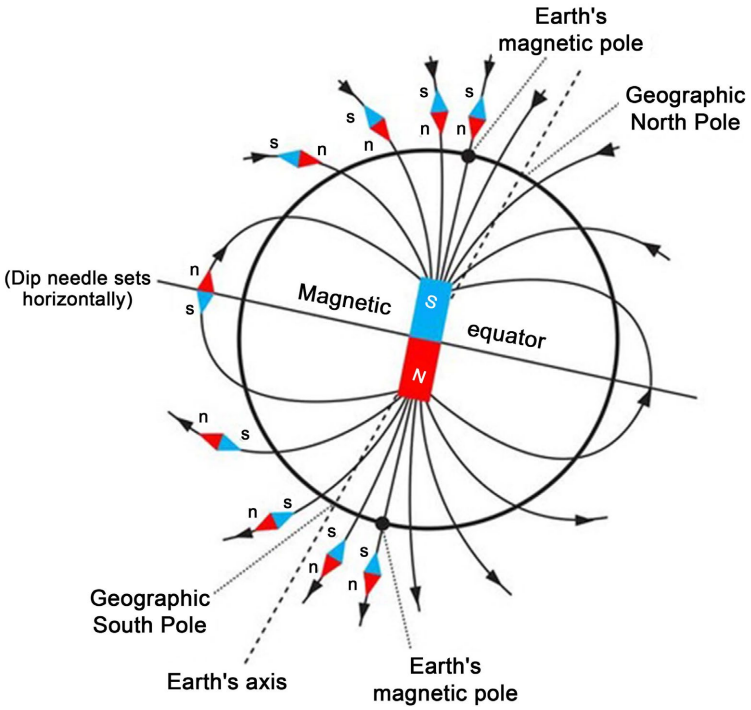

Figure 9. Close up depiction of the Earth's geomagnetic field lines [13] relative to surface of the Earth [12].

The measurement of the magnetic field on the ground of the Earth also has a specific advantage in that the data are not affected by the parasitic magnetic field in the ionosphere caused by the solar wind and ionized particles along the path of the satellite.

The basic equation of the force between two different permanent magnet poles q_{m1} and q_{m2} is given by:

$$F = \frac{\mu_0 q_{m1} q_{m2}}{4\pi r^2} \tag{5-2}$$

which is formally equivalent to the equation for the force between two electrostatic

charges [45]-[47][9].

To determine the magnetic strength of the test magnets, F_1 was measured at the moment when each half of the full length of the test magnets was pulled to be separated at the preset separation gap distance r_1. From the randomly chosen separation distances of r_1 5.2 mm and 5.1 mm, 1.2 kg and 0.65 Kg of weight equivalent horizontal magnetic pulling forces were measured respectively

$$F_1 = \frac{\mu_0 q_m q_m}{4\pi r_1^2} \tag{5-3}$$

to estimate the magnetic charge strengths of the two test magnets. It was determined that using this method to measure the strength of each magnetic pole is more direct and reliable than using the result of the magnetic flux density measured by a Gauss meter and converting it into the magnetic charge strength using the mathematical relation. This method avoids the calibration dependency error caused by magnetometers that use the strength of the Earth's geomagnetic field, which changes depending on the time and location for calibration.

The next step is to measure the strength of the magnetic force from the monopole charge of the Earth and calculate the estimated number of neutrons in the entire Earth to obtain the single magnetic monopole charge of the individual neutrons and subsequently that of the individual neutrinos.

For the total magnetic monopole charge Q_m of the Earth, the tilting force due to the interaction between the Earth's magnetic monopole and the dipole magnet placed on the horizontal pivot at the center is given by

$$F_2 = \frac{2\mu_0 q_m Q_m}{4\pi R^2} \tag{5-4}$$

The factor of 2 comes from the two sides, one from the attractive force between N and S and the other from the repulsive force between N-N on the opposite side of the test magnet.

The elevation of the test site in the city of Cuenca Ecuador is 2.56 km above sea level.

Therefore, $R = (6368 + 2.56)\text{km}$ and the downward tilting weights measured repeatedly at the horizontal position of the magnets turned out to be (0.78 ± 0.04) g and (0.52 ± 0.03) g respectively, on the digital micro scale for the two test magnets.

5.3.2. Measurement and Relevant Data

Rod magnet	Length	Diameter	F_1	r_1	F_2	B_0	Weight R/L	
Rod magnet 1	16.6 cm	12 mm	1.2 kg	5.2 mm	0.78 g	454 mT	71.83 g/71.84 g	(5-5)
Rod magnet 2	19 cm	10 mm	0.65 kg	5.1 mm	0.52 g	413 mT	56.83 g/56.85 g	

[9]International Association of Geomagnetism and Aeronomy, Working Group V-MOD. Participating members, C. C. Finlay, S. Maus, C. D. Beggan, T. N. Bondar, A. Chambodut, T. A. Chernova, A. Chulliat, V. P. Golovkov, B. Hamilton, M. Hamoudi, R. Holme, G. Hulot, W. Kuang, B. Langlais 12 October 2010 https://doi.org/10.1111/j.1365-246X.2010.04804.x "International Geomagnetic Reference Field: the eleventh generation". *Geophysical Journal International.* 183 (3): 1216-1230.

The south pole sides of the magnets were pulled down consistently for both Rod Magnet 1 and Rod Magnet 2, indicating that the Earth is a north magnetic monopole. "Weight R/L" is the weight of half of each test magnet separately measured before assembling the two halves into the full length.

5.3.3. Total Magnetic Monopole Charge from the Earth

Using the data collected after repeated measurements, we found $Q_m = (2.75 \pm 0.14) \times 10^{16}$ Weber for the Earth's monopole magnetic charge of the north type measured by Rod Magnet1 and $Q_m = (2.54 \pm 0.13) \times 10^{16}$ Weber for the same north type measured by Rod Magnet2. The average of the two measured values $Q_m = (2.65 \pm 0.13) \times 10^{16}$ Weber was determined for the north magnetic monopole charge of the Earth.

Two different sets of test magnets were employed to eliminate spurious experimental results when only a single set of test magnets was used. The two permanent magnet bars were not of the same brand or of the same diameter or length. Despite the deliberate choice of two entirely different sets of test magnets, the experimental results were unexpectedly close to each other.

To estimate the magnetic field at the surface of the earth stemming from the measured magnetic charge of the earth $Q_m = (2.65 \pm 0.13) \times 10^{16}$ Weber at the distance $R = (6368 + 2.56)\,\text{km}$, we use the magnetostatic force Equation (5-2)

$$F = \frac{\mu_0 Q_m q_m}{4\pi r^2} \tag{5-6}$$

where Q_m represents the total magnetic charge of the earth, q_m is the test magnetic monopole charge placed on the surface of the earth, and because $\mu_0 / 4\pi = 10^{-7}$, the magnetostatic force is given by

$$F = 10^{-7} \frac{2.65 \times 10^{16} \times q_m}{\left(6370.56 \times 10^3\right)^2} = 65.3\ \mu\text{T} \times q_m \tag{5-7}$$

This result shows that the strength of the magnetic monopole field at the surface of the Earth at the equator, owing to the magnetic monopole charge of the Earth, is estimated to be approximately 65.3 μT. Past measurements [48] of the Earth's geomagnetic field from the SWARM satellite were in the range of 25 μT near the equator and 65 μT near the pole. The satellites actually measured both the Earth's magnetic monopole and the geomagnetic dipole field together in orbit because there are no means to measure them separately. The Earth's magnetic monopole field strength adjusted at a height of 510 Km above sea level is approximately 56 μT according to the result (5-7). This is very close to the generally accepted Earth magnetic field strength 50 μT measured by satellites. Because the two methods of earth magnetic field measurement are completely independent of each other, the agreement in the order of the magnitude of the Earth magnetic field strength at the equator is considered significant. We used the magnetometer only to choose an identical disk magnet to be placed at the end of the test bar magnet to ensure that the magnetic fields at the tips were identical in strength. This minor differ-

ence could be caused by the fact that the laboratory magnetometers used in the satellite are calibrated based on the geomagnetic field of the Earth, which is known to fluctuate depending on time and location.

5.3.4. Total Number of Neutrons on the Earth

To estimate the total number of neutrons on Earth to calculate the individual magnetic monopole charge of the neutron, the element table [49] was utilized.

According to the element table, the following distribution applies to 99.9 percent of the mass on Earth's elements:

%	Element	# Neutron/Proton	Weighted average N/P
5.63	Iron	30/26	168.9/146.38
46.1	Oxygen	8/8	368.8/368.8
28.2	Silicon	14/14	394.8/394.8
2.33	Magnesium	12/12	27.96/27.96
8.23	Aluminum	14/13	115.22/106.99
4.15	Calcium	20/20	83/83
2.36	Sodium	12/11	28.32/25.96
2.09	Potassium	20/19	41.8/39.71
0.565	Titanium	26/22	14.69/12.43
0.095	Manganese	30/25	2.85/2.375
0.14	Hydrogen	0/1	0/0.14

(5-8)

The mass difference due to the isotopes was included in the average atomic mass of each element. Subsequently, we find the percentage distribution of the mass of the Earth to be 50.7% neutrons and 49.3% protons, and the contribution from electrons is negligible. Using the known total mass of Earth 5.972×10^{24} kg and the mass of a single neutron 1.675×10^{-27} kg, the best estimated number of neutrons on Earth was determined to be $\#n_{earth} = 1.8076 \times 10^{51}$.

5.3.5. Magnetic Monopole Charge of a Single Neutrino

From these results, the single magnetic monopole charge m_ν of the neutron

$$m_\nu = \frac{Q_m}{\#n_{earth}} = (1.46 \pm 0.07) \times 10^{-35} \text{ Weber} \tag{5-9}$$

is determined with a 95% confidence level, which is the same as that of the neutrino based on the principle of universal charge conservation. This level of strength of the magnetic charge of the neutron is out of the range of the single neutron magnetic monopole charge detection method that may have been attempted in the laboratory. Neutrons pass through a single slit and are subjected to a strong magnetic field perpendicular to their path, which may be used to detect the deviation of their path from that without a magnetic field. However, there are no re-

ports of this type of experiment being performed on neutrons. The key issue in such an experiment is the possibility of obtaining the highest strength of the perpendicular magnetic field versus the accuracy of the measurement of the deviation of the neutron path from that without the magnetic field.

Experiments were also performed on the opposite side of the globe in Pontianak (0.03109˚S, 109.32199˚E) Indonesia, Bangkok (13.7524˚N, 100.5507˚E), and Chengdu (30.6593˚N, 104.0598˚E), China. The same northern magnetic monopole charge on Earth was observed in Pontianak at 0.03109˚S. The experiment performed in Bangkok showed a zero tilting effect on the balanced test bar magnets, indicating that 13.7524˚N latitude is where the effect from the north magnetic monopole effect of the Earth cancels the south magnetic pole component of the Earth's geomagnetic field. In Chengdu, 30.6593˚N, a strong geomagnetic field effect of the south pole component (note: Earth's North Pole is magnetic south pole) was observed to override the monopole effect.

Further investigation showed that the repulsive monopole magnetic force between two matter objects was 1.14×10^{-13} times small than the attractive gravity force between them, assuming that the same number of neutrons comprised each of the two matter objects. This indicates that the repulsive magnetic monopole forces among stars and planets are extremely weak and negligible compared to that of gravity on a planetary or galactic scale.

5.3.6. Comparison with Dirac's Predicted Magnetic Monopole Charge

The discrepancy between this finding and the results of past studies is that the measured magnetic monopole charge of the neutron does not match Dirac's prediction of $g = \frac{N}{2}\frac{\hbar c}{e}$ [50], where $\hbar$ is Planck's constant and N is an integer resulting in the calculated Dirac's magnetic monopole charge $N \times 0.99 \times 10^{-7}$.

However, if Dirac's magnetic monopole is used for the magnetic monopole charge of a neutron, the repulsive magnetic force between matter objects becomes too large to be ignored in celestial mechanics. A Newtonian mechanical description of planetary motion does not apply in such cases.

There is a difference in the order of 10^{28} between Dirac's and the present report of the magnetic monopole charge 1.46×10^{-35} Weber. Dirac's magnetic monopole charge is close to the value $g = N\frac{\mu_0}{4\pi}$ where $\mu_0 = 4\pi \times 10^{-7}$ H/m is the vacuum permeability.

5.3.7. Vacuum Permittivity and Magnetic Monopole Charge Connection

The measured magnetic monopole charge of a neutron coincides with the value of the vacuum permittivity divided by Avogadro's number.

$$8.854 \times 10^{-12} \left(\text{Faraday/Meter}\right) / 6.022 \times 10^{23} = 1.47 \times 10^{-35} \text{ Weber} \qquad (5\text{-}10)$$

A possible reason is that while the vacuum permittivity ε_0 is generally perceived to be associated with the electric field, the Coulomb electric field is inversely

proportional to ε_0 because of the $\frac{1}{4\pi\varepsilon_0}$ factor, whereas ε_0 and μ_0 are mutually constrained by the relation $c=\frac{1}{\sqrt{\varepsilon_0\mu_0}}$, which suggests that although ε_0 has the unit *Faraday/Meter*, the vacuum permittivity is directly related to the strength of the magnetic monopole charge density in space.

5.4. Neutron Beta Decay Process Including Magnetic Monopoles

Based on the principle of charge conservation in the universe, including both electric and magnetic charges, the full neutron beta decay process can now be expressed as:

$$ {}_{0}^{1}n_{1} \to {}_{1}^{1}p_{0} + {}_{-1}^{0}e_{0} + {}_{0}^{0}\overline{\nu}_{e1} \tag{5-11} $$

where the low right-hand side subindices indicate the number of conserved magnetic monopole charges. In this figure, the W boson is identified as a temporary composite transient state of the particle that has both magnetic and electric charges before splitting into the electron and antineutrino. As J. J. Steyaert pointed out in his paper, the weak interaction in the standard model could be a manifestation of the magnetic monopole effect in nuclear interaction processes. This new result of the existence of a non-zero magnetic monopole charge prompts Maxwell's equations to be modified to include the full spectrum of magnetic monopole phenomena that manifest in the universe.

5.5. Symmetric Form of Maxwell's Equation

We propose the symmetric form of Maxwell's Equations (5-12) which is based on the experimental confirmation of the magnetic monopole in the form of a neutron's static charge and the magnetic current of the traveling neutrinos,

$$ \begin{aligned} &\nabla\cdot\boldsymbol{E}=\frac{\rho_e}{\varepsilon_0} \\ &\nabla\cdot\boldsymbol{B}=\mu_0\rho_m \\ &\nabla\times\boldsymbol{E}=-\frac{1}{\varepsilon_0}\frac{\partial\boldsymbol{B}}{\partial t}-\frac{1}{\varepsilon_0}\boldsymbol{J}_m \\ &\nabla\times\boldsymbol{B}=\mu_0\boldsymbol{J}_e+\mu_0\frac{\partial\boldsymbol{E}}{\partial t} \end{aligned} \tag{5-12} $$

where ρ_m is the static magnetic monopole charge density formed by neutrons and $\boldsymbol{J}_m$ is the magnetic monopole current density from the traveling neutrinos. Other researchers have reported similar forms of the symmetric Maxwell's equation [51]. The conventional expression $\nabla\cdot\boldsymbol{B}=0$ in the original Maxwell's equation passed the experimental test without measurable inconsistency because the magnetic charge density ρ_m is extremely weak and individually undetectable unless the collective effect from a large number of neutrons is subjected to the test. The current density $\boldsymbol{J}_m$ in the third equation does not have a net value in homogeneous isotropic space because of the isotropy of the neutrino flux, despite the

massive number of its presence in the universe, which explains the absence of this term in the original Maxwell's equation.

Magnetic current is observable in the form of magnetic flux when a coherent collimated stream of magnetic monopole neutrinos passes along the magnet, forming an air-gap loop. The actual effect of the electrical current in a typical copper magnet wire according to Equation (5-12) is to rearrange the flow of the random magnetic current that already exists in space into a coherent collimated stream instead of creating the entire magnetic flux from the empty space.

Maxwell's equations have not been found to violate any known physical phenomena, but questions remain as to why the equations are not symmetric with respect to magnetism and why there are no individual magnetic monopoles.

5.6. Atomic Stability Condition and the Estimated Speed of the Magnetic Monopole Neutrinos in the Universe

5.6.1. Electric Field Created by Traveling Magnetic Monopoles

The symmetric Maxwell's Equation (5-12) provides a new solution for the electric field created by the traveling magnetic monopole neutrino, which is given by

$$\boldsymbol{E} = -\frac{1}{4\pi\varepsilon_0}\frac{m_v \boldsymbol{\upsilon}\times\hat{r}}{r^2} \tag{5-13}$$

where m_v is the single magnetic monopole charge and $\boldsymbol{v}$ is its velocity. This result is a mirror image of the solution of the magnetic field created by the moving electric charge in the original Maxwell's equations. According to the classical electrodynamic description of atoms, orbiting electrons radiate photons, lose energy, and collapse into the nucleus, which is the cause of the development of quantum mechanics. The core of the puzzle is how the electrons stay afloat from the nucleus and avoid collapse, especially those in the s orbital, which has zero angular momentum, assuming that the exchange of photon energy allows electrons with non-zero angular momentum to stay in the orbit. The quantized photonic energy relation $E = h\nu$ originates from the property of the vacuum space without reference to the presence of nearby electrons. As such, there is a possibility that some unknown external electric fields in space could counteract the attractive Coulomb force between the nucleus and electron. In fact, the electric field (5-13) created by traveling magnetic monopole neutrinos could be a candidate source of such an external electric field.

In the absence of a viable mechanical picture of the behavior of electrons in atoms, we propose that the electric fields (5-13) created by traveling magnetic monopole neutrinos in space are responsible for the stability of atomic structures. The validity of this proposition depends on its ability to address physical details in the understanding of the universe in accordance with numerical and observational data.

5.6.2. Electromechanical Atomic Stability Condition

To maintain atomic stability, the vacuum electric field (5-13) created by the traveling magnetic monopole neutrinos must have equivalent strength to the Cou-

lomb electrostatic field of the proton

$$E = \frac{1}{4\pi\varepsilon_0}\frac{e}{r^2} \tag{5-14}$$

to prevent electrons from collapsing into protons based on the electrodynamic principle.

The two electric fields (5-13) and (5-14) are of different geometrical types because one (5-13) has a cylindrical geometry and the other (5-14) is radial in spherical form. However, depending on the frequency of the large number of directionally varying magnetic monopoles passing by the proton, the two fields counteract each other and maintain the electron in a constant agitating and rotating state. The unique combination of these two geometrically different electric fields creates enormous complexity owing to the large number of randomly traveling background neutrinos. In all these cases, unless the order of magnitude of the strengths of the electric field (5-13) and (5-14) are within the same range, the electron will either collapse into the proton or fly away from the boundary of the atomic orbit.

5.6.3. Estimated Speed of Magnetic Monopole Neutrinos in the Universe

By equating the electric field (5-13) at $\theta = 90^\circ$ ($\boldsymbol{v} \perp \boldsymbol{r}$) and (5-14), the optimum speed of the magnetic monopoles to prevent the collapse of the electron-proton substructure is

$$\upsilon = \frac{e}{m_v} \tag{5-15}$$

For the charge of an electron $e = 1.6021766 \times 10^{-19}$ Coulomb and the measured magnetic monopole charge $m_v = 1.46 \times 10^{-35}$ Weber we find the speed of the magnetic monopole neutrino 1.098 × 10^{16} m/sec, which is 3.655 × 10^7 times the speed of light to be able to stabilize the hydrogen atom and/or all the atoms since there is no dependency on r in the relation (5-15).

This result indicates that the calculated speed of the background neutrinos needed to stabilize the atomic structure is universally identical regardless of the specific atomic numbers or where the atom is located. This particular speed of is necessary to maintain the stability of the entire architecture of the material universe without having to resort to quantum mechanical uncertainty according to this particular electromechanical model.

In fact, the negative mass squared problem of neutrino experiments reported by five major institutions have prompted the suspicion that neutrinos may not be ordinary matter particles. Stationary neutrinos have not been detected thus far, which is necessary to prove that neutrinos are ordinary matter particles. In addition, there is no evidence that right-handed neutrinos are most likely to be observed if neutrinos can be stationary [52][10]. Neutrinos have the unusual property of mass oscillation between flavors, which has not been observed in electron fam-

[10]Backe H. *et al.*, Nucl. Phys. B (Proc. Suppl.) 31, 46(1993); Stoeffl W., Bull. Am. Phys. Soc. 37, 925(1992); Kawakami H. *et al.*, Phys. Lett. B 256, 105(1991); Holzschuh E. *et al.*, Phys. Lett. B 287, 381(1992); Wilkerson J. F. Nucl. Phys. B (Proc. Suppl.) 31, 32(1993).

ilies. Despite the recent success in the detection of the non-zero rest mass of neutrinos, there are too many inconsistencies to fit neutrinos into the category of the ordinary inside light cone particles, and that the simplest possible way to resolve the mystery of neutrinos may be to change our point of view and determine that neutrinos are actually tachyons. The most glaring inconsistency is in the fact that the vast majority of the 10^{79} neutrinos in the universe are not detectable, and few of the detected neutrinos have a speed close to the speed of light, which does not necessarily prove that the rest of the neutrinos would also be traveling close to the speed of light because neutrinos, as fermions, are not required to have a fixed speed of travel. If most of them are not stationary, based on the fact that stationary state neutrinos have not been detected, the only possibility is that the vast majority of them must be traveling much faster than the speed of light, which is consistent with the negative mass squared problems reported by the earlier experimental results. As such, despite the questionable possibility that background neutrinos could travel 3.655×10^7 times the speed of light, we proceed to further investigate what else can be found from the same proposition.

5.7. Vacuum Electric Field, Quantum Mechanical Uncertainty and Dark Energy

5.7.1. Vacuum Electric Field

The vacuum electric field $\boldsymbol{E}(\boldsymbol{r},t)$ created by the fast-traveling magnetic monopole tachyonic neutrinos in the background is given by:

$$\boldsymbol{E}(\boldsymbol{r},t)=\sum_{i=1}^{N}\frac{1}{4\pi\varepsilon_0}\frac{m_v\boldsymbol{\upsilon}_i\times\left(\boldsymbol{r}-\boldsymbol{r}_i(t)\right)}{\left|\boldsymbol{r}-\boldsymbol{r}_i(t)\right|^3} \tag{5-16}$$

which is a multiple sum of the individual electric fields (5-13), where m_v is the magnetic monopole charge of the neutrino, $\boldsymbol{v}_i$ is the velocity, $\boldsymbol{r}_i(t)$ is the position of the particle at time t and N is the total number of neutrinos in the universe which is estimated to be in the order of 10^{79} [53].

5.7.2. Repulsive Potential Energy Created by Magnetic Monopole Neutrinos

The uniformly distributed superluminal magnetic monopole neutrinos accumulate repulsive magnetic potential energy in space, which is expressed in the following differential form:

$$\mathrm{d}U_r=\frac{\mu_0\rho_m\left(\frac{4}{3}\pi r^3\right)}{4\pi r}\mathrm{d}\left(\rho_m\left(\frac{4}{3}\pi r^3\right)\right) \tag{5-17}$$

where ρ_m is the magnetic monopole charge density at the universe.

The calculation of U_r over the radius of the observable universe identifies the repulsive magnetic potential energy from the uniformly distributed magnetic monopole neutrinos, given by

$$U_r=\frac{3\mu_0N^2m_v^2}{20\pi R}\text{Joule} \tag{5-18}$$

where R is the radius of the observable universe 4.4×10^{26} meter [54], N is the total number of magnetic monopole neutrinos, which is of the order of 10^{79} and m_v is the single magnetic monopole charge 1.46×10^{-35} Weber and $\mu_0 = 4\pi\times10^{-7}$ H/m , and the vacuum energy in this particular case is $U_r = 2.907\times10^{54}$ Joule .

Because nature tends to move toward the lowest energy state whenever possible, the universe must expand to reduce its repulsive vacuum potential energy, according to the result (5-18).

5.7.3. Total Energy Created by the Electric Field Carried along by Traveling Magnetic Monopole Neutrinos

There is also energy created by the interaction of the electric fields carried along by the traveling magnetic monopoles, represented by (5-13). For example, when two neutrinos travel in a parallel trajectory, there is a repulsive electric force perpendicular to both the direction of their travel and the line connecting the two neutrinos, because the directions of the two cylindrical electric fields run against each other. In addition, when two neutrinos travel in opposite directions passing each other in a parallel trajectory, there is an attractive interaction perpendicular to both the direction of their travel and the line connecting them. As such, any type of interaction between the electric fields generated by traveling magnetic monopoles does not directly contribute to either attraction or repulsion between the neutrinos themselves, while they still create energy. In general, energy is related to either attraction or repulsion among material objects in both gravitation and static electromagnetism, but this is a new form of energy because the lines of force do not connect the two objects in action.

The energy created by these interactions is represented by

$$\mathrm{d}U = \frac{m_v n\upsilon\frac{4}{3}\pi r^3}{4\pi\varepsilon_0 r}\mathrm{d}\left(m_v n\upsilon\frac{4}{3}\pi r^3\right) \tag{5-19}$$

where n is the number density of neutrinos in space, m_v is the magnetic monopole charge of the neutrino, and υ is the speed of the traveling background neutrinos. By integrating (19) over the radius R (4.4×10^{26} meter) of the observable universe, the total electric vacuum energy of the universe is found:

$$U_{electric} = 3.13\times10^{103}\ \text{Joules} \tag{5-20}$$

We identify this energy as the main component of the dark energy that does not directly contribute to the expansion; however, it supports the structural integrity of the material universe. From the perspective of quantum field theory, the fact that the force lines of this interaction do not directly connect the two objects in motion, yet they accumulate a large amount of energy in space, is consistent with the fact that photons as bosons in quantum field theory do not obey Pauli's exclusion principle because they are created by traveling tachyonic magnetic monopoles (fermions) as spiraling electric fields according to Maxwell's equation.

5.7.4. Strength of Vacuum Electric Field

Using the relation $\frac{U}{\frac{4}{3}\pi R^3} = \frac{1}{2}\varepsilon_0 E^2$ we obtain the strength of the vacuum electric field (5-16) given:

$$|E| = 1.41\times 10^{17} \text{ Newton/Coulomb} \tag{5-21}$$

Considering that the rigidity of the medium determines the upper limit of the frequency of the waves it carries in general, this is considered a strong vacuum electric field as a medium for handling ultra-high-frequency electromagnetic waves propagating in space. The rapidly fluctuating background electric field has the same average strength as the Coulomb electric field at a distance 10^{-13} m from the proton, which is larger than the proton's charge radius 8.4×10^{-16} m but smaller than the Bohr radius 5.3×10^{-11} m, which serves both as a mechanism for quantum fluctuation and as a medium for electromagnetic wave propagation in space traditionally known as ether.

5.7.5. Origins of Quantum Mechanical Uncertainty and Non-Locality

The equation of motion of a free electron in a vacuum using a vacuum electric field (5-16) is written as

$$m_e \frac{\mathrm{d}^2 \boldsymbol{r}}{\mathrm{d}t^2} + \frac{e}{4\pi\varepsilon_0}\sum_{i=1}^{N} \frac{m_v \boldsymbol{\upsilon}_i \times \left(\boldsymbol{r} - \boldsymbol{r}_i(t)\right)}{\left|\boldsymbol{r} - \boldsymbol{r}_i(t)\right|^3} = 0 \tag{5-22}$$

which defines the inertial mass of an electron in vacuum. The motion of a charged particle in free space is restricted by the presence of a rigid fluctuating electric field; however, the particle's position and momentum are not precisely determined on the microscopic scale.

The quantum particle's position and momentum in free space are under constant interference of the magnetic monopole current of neutrinos that have random motion characteristics. This indicates that in addition to the contribution to dark energy, the stochastic interaction between the traveling magnetic monopole neutrinos and charged particles causes quantum mechanical uncertainty of position and momentum without apparent external forces of known origin.

Subsequently, we write the full equation of motion of an electron in an isolated hydrogen atom in space as:

$$m_e \frac{\mathrm{d}^2 \boldsymbol{r}}{\mathrm{d}t^2} + \frac{e}{4\pi\varepsilon_0}\sum_{i=1}^{N} \frac{m_v \boldsymbol{\upsilon}_i \times \left(\boldsymbol{r} - \boldsymbol{r}_i(t)\right)}{\left|\boldsymbol{r} - \boldsymbol{r}_i(t)\right|^3} + \frac{e^2}{4\pi\varepsilon_0 r^2} = 0 \tag{5-23}$$

where m_e is the mass of the electron, and e is the single electronic charge.

Equations (5-22) and (5-23) may be reduced into probabilistic statistical forms to obtain meaningful physical information on the electron because there are no means to predict the precise motions of each individual tachyonic magnetic monopole neutrino in the universe other than the physical constraints that they are expected to observe collectively. A mathematical reduction of Equations (5-22) and (5-23) into probabilistic forms, the task of which is beyond the scope of the present

report, is expected to result in a formal structure reminiscent of the Schrödinger equation when the following constraints are applied:

In general, fermions do not have a fixed speed of travel, and a case was projected where tachyonic magnetic monopole neutrinos have a Maxwell-Boltzmann type velocity distribution, such as gas molecules peaking around 1.095×10^{16} m/sec and tapering off to zero at both the speed of infinity and speed of light at the low end. However, because tachyonic neutrinos do not have inertial mass, such as matter particles, nor their motion is influenced by ambient temperature, it is concluded that their velocity distribution must be radically different and close to a delta function peaking at 1.095×10^{16} m/sec in addition to the isotropic condition $\sum_{i=1}^{N} m_{\nu} \boldsymbol{\upsilon}_i = 0$.

On the other hand, the arguments against the legitimacy of quantum mechanics, for example, action at a far great distance, non-locality, quantum entanglement, hidden variables, and incompleteness of quantum mechanics [55], are expected consequences of the theoretical efforts to incorporate the inherent interference from the superluminal tachyonic magnetic monopoles in space that is missing in the local probabilistic description of classical quantum mechanics because 3.655×10^{7} times the speed of light is almost instant to reach the far side of the universe in a practical sense.

5.8. Cause of the Absence of Measurable Single Magnetic Poles

Owing to the duality of electricity and magnetism in Maxwell's equations, regardless of the presence of a magnetic field, there must be an electric current loop creating the two poles of the magnetic field at the macroscopic scale. If two poles of the dipole magnet are created by the traveling magnetic monopole particles, the division of the dipole magnet in half will not create two magnetic monopoles. The two different magnetic poles are composed of incoming and outgoing magnetic monopole neutrino fluxes. If a monopole magnet stays close to the outgoing magnetic monopole, it will be repelled; however, if it stays on the incoming side of the magnetic flux, the magnetic monopole will be attracted to the magnet. Contrary to the case of electrons that can stay at rest, because magnetic monopole neutrinos can never be in a stationary state, an isolated single magnetic pole cannot be found at the macroscopic scale. Conventional Maxwell's equations describe that the physics of electricity and magnetism works well even in the absence of magnetic monopoles in the universe. However, due to the universal charge conservation principle, if neutrinos have magnetic monopole charge, neutrons must also have magnetic monopole charge. The present report is based on this assumption, and it turns out that neutrons have a very small magnetic monopole charge. In effect, the direction of the stream of the magnetic monopole neutrino flux passing through the looped electronic current inside the metallic magnet determines which side is N and which side is the inseparable S pole of the magnet. In essence, the strength of the magnetic field at the macroscopic scale originates from the inherent superluminal speed of the magnetic monopole neutrinos, as shown in the solution of

the modified Maxwell's Equation (5-13). On the other hand, the extremely weak strength of the single magnetic monopole charge of the (stationary) neutrons resulted earlier searches into the conclusion that there are no observable magnetic monopoles in the universe. Therefore, it was necessary to measure the bulk effect of the magnetic monopole charge from the massive number of neutrons and divide the measured result by the total number of neutrons present on earth, which showed that the single magnetic monopole charge is immeasurably small to be detected individually.

5.9. Discussion

The prediction of the expanding universe and calculation of the dark energy using the quantum stability condition (5-15) were not intended objectives at the start of this investigation. We investigated the mechanical stability of the atoms using the solution from the new symmetric Maxwell's equations based on the measured magnetic monopole charge of neutrinos. The behavior of the electrons in the s-orbital prompted the proposition of the atomic stability condition using a new solution of the electric field created by traveling magnetic monopoles.

The incredibly fast speed of travel of these particles ensures their uniform density in a vast space and creates large sums of vacuum energy owing to the interactions among the neutrino's velocity-induced electric fields (5-13). The existence of stable atomic structures and the material universe is not compatible without such a paradoxical arrangement because the undetermined mechanical aspect of quantum uncertainty is supported by the electric fields created by the traveling background magnetic monopole neutrinos, which is the basis of the existence of the material universe.

In the most recent development, neutrinos were observed to change flavors while traveling in space, especially when they emerged out of the South Pole of Earth, according to a recent experimental report [56]. Because the neutrino's magnetic monopole is of the north type, the background neutrinos in space are pulled into Earth's North Pole (which is magnetic south pole), pass through Earth's rotation axis, and exit the South Pole with changed flavor and gained energy, which explains the experimental result. This means that the neutrinos that disappeared into the background after losing energy came back to be detected because of the energy-exchange interactions between the traveling north magnetic monopole neutrinos and Earth's geomagnetic field. This experimental result suggests that it is not the mass, but the magnetic monopole charge of the neutrinos that activates neutrinos to gain energy and change flavors. It was also reported that the solar wind tends to move more toward the North Pole than toward the South Pole, which is a mystery. The mystery may be resolved if the two neutrons (as north magnetic monopoles) inside the helium ion nuclei, which comprise one of the major components of the solar wind, are attracted toward the North Pole (south magnetic pole) and repelled by the South Pole (north magnetic pole).

Conclusion

We tested the hypothesis that neutrons could have a magnetic monopole charge by measuring the collective effect from the massive number of neutrons inside the Earth on two accurately balanced test bar magnets. Following the definite result of the neutron's magnetic monopole charge from the measurement, we generalized Maxwell's equation to a symmetrical form because the charge conservation principle dictates that neutrinos must also have a magnetic monopole charge.

Assuming that quantum particles must have a certain level of kinematical aspects in their behavior in addition to the statistical ones, we postulated that many of the background neutrinos would affect the dynamics of the electrons orbiting the nucleus. This was considered natural because traveling magnetic monopoles generate a spiraling electric field on their paths, according to the symmetric form of Maxwell's equation. The strength of the electric field created by the traveling magnetic monopoles should be comparable to the binding energy of the electrons in the atomic structures in s-orbit to guarantee a stable atomic structure and, consequently, the universe. From this result, we concluded that the stochastic nature of the quantum phenomena is due to the random motion of the background neutrinos creating chaotic electric field in vacuum, "stabilized" due to their uniform density. This pervading invisible and undetectable random electric field in space is also identified as the essence of the medium for electromagnetic wave propagation, known as ether. We subsequently obtained a mathematical expression for the energy created by the pervading electric field caused by traveling neutrinos, which matches the estimated dark energy reported by other researchers.

The speed of neutrinos was calculated without prior restriction from the result of special relativity because Maxwell's equation has no previous record of having failed any experimental test. While the speed of light limit applies to matter particles that obey the Newtonian mechanical principle, there is no evidence showing that neutrinos have the same mechanical properties as matter particles that follow Newton's law of motion, since stationary neutrinos have never been found despite the sheer number of their existence in the universe. The previous experimental measurement of the non-zero mass of neutrinos does not necessarily prove that neutrinos can be stationary. Since the first law of Newtonian mechanics states that "a body continues in its state of rest, or in uniform motion in a straight line, unless acted upon by a force," there must be a verifiable existence of stationary state, because the object can be subjected to a Newtonian mechanical principle. The absence of a stationary state of neutrinos means that neutrinos cannot be subjected to special relativity; therefore, the imposition of the speed of light limitation onto neutrinos was an overreach generalization that it did not have its original compass. In addition, from a practical technological point of view, the property of the vacuum space filled with tachyonic magnetic monopole neutrinos could provide us with a clue on how to maneuver the vast space of the universe without having to rely on conventional propulsion technology, considering that the understanding of the physical property of the medium that needs to be acquired is the first step in finding the key for the necessary technology.

Reflection

After accidentally noticing the significant tilting of the compass needle in the high-latitude geographical regions of the Earth in 2017, we suspected that there must be some kind of geocentric magnetic field that affects the balance of the compass needle because the compass manufacturers will not roll out their compasses in such an unbalanced state. Because we have wondered why there are no magnetic monopoles in the universe, it came to the conclusion that if there is a magnetic monopole field emanating from the Earth by the massive number of neutrons, the tilting effect of the balanced test bar magnet due to the vertical component of the geomagnetic field must be isolated by all means to accurately account for the Earth's collective magnetic monopole field originating from all the neutrons. This event spurred the decision to perform the experiment to detect the Earth's magnetic monopole field. The first author is grateful to his mentors of the early days who taught him the wonders of mathematics and physics.

This is an unexpected confirmation because not only is the presence of magnetic monopoles verified, but also because the measured individual magnetic monopoles play the role of a physical entity that dominates all other matter particles that have real mass in the universe, especially because of their sheer numbers and speed of travel. It certainly appears that they are present at any time at any place almost at the same time in the universe, causing the ubiquitous quantum effect. The fact that the number of unsolved physics mysteries has been reduced by the discovery of magnetic monopole tachyonic neutrinos is particularly interesting. We can see the possibility that this background tachyonic magnetic monopole neutrino could also be the fundamental cause of gravity. Considering that neutrinos are one of the byproducts of the weak decay of neutrons, there is ample reason to believe that this background tachyonic magnetic monopole neutrino is behind the weak interaction phenomenon in elementary particle physics. As such, it is possible that W and Z bosons are composite particles of neutrinos, electrons, and positrons that exist momentarily in space.

6. Possible Manipulation of Outgoing Magnetic Field as a Method for Space Travel

When a massive object remains in free space, the background neutrinos have uniform obstructions from all directions to pass through the object. The flux of the background neutrinos forms the source of the force that moves the object. When the forces from all directions are the same, the object remains in the same position, except that the object can move at a constant speed. This is the force from all directions canceled by the object. When a massive object of mass M remains in space, the surrounding area is obstructed by the passage of neutrinos. The motion of the object in space is considered negligible compared to the speed of each background neutrino.

The direction of the gravitational force is where the massive object is headed. The further the distance from it, the fewer the number of obstructions in the flow

of tachyonic magnetic monopole neutrino flux and the less force. The dispersion of the magnetic flux is spread throughout $4\pi r^2$, where r is the distance between two matter objects.

The magnetic monopole neutrino flux density multiplied by the interaction cross-section is the force that the tachyonic magnetic monopole neutrinos can exert on the mass of the particle placed in empty space. When there is no gravitational effect nearby, the object is in a neutralized state of external force owing to the isotropy and homogeneity of space. However, when the isotropic flux stream is blocked by the presence of a massive object, the flux density is reduced proportionally to $1/(4\pi r^2)$, which is the surface area of the flux dissipating throughout three-dimensional space. As the distance between the two gravitating masses increases, the effect of the magnetic neutrino flux blockage diminishes, and the flux around the test object returns close to an empty space.

The magnetic monopole tachyonic neutrinos bounce off the hadrons because they are impenetrable balls of random magnetic field owing to the chaotic motion of the quarks and the accompanying gluons. Consequently, the flux of the isotropic neutrino flux spreads uniformly at spatial angles.

How can the universal gravitational constant be related to the magnetic monopole charge or speed? The gravitational constant factor must be related to the density of the tachyonic magnetic monopole neutrinos and the momentum carried by individual neutrinos. Magnetic repulsion force between hadrons and tachyonic magnetic monopole neutrinos and background neutron number density.

The isotropy of background neutrinos causes no net motion on the test object, which is the cause of the momentum conservation principle, which is also called the flat space time of empty space in general relativistic expression. The momentum conservation principle in mechanics holds true because the net external force on the test object is zero. The presence of a massive object that disperses the neutrino flux prevents the test object from obtaining an isotropic balance of force in space, which causes the object to be pushed toward the gravitational center of the massive object located nearby. It is noted that when magnetic monopole neutrinos are involved in physical interactions, it becomes a quantum phenomenon in the traditional sense of understanding quantum mechanics. Because quantum mechanics is a pure manifestation of the physical effect of tachyonic magnetic monopole neutrinos on number of protons and hydrogens to form multiple electrostatic bonding to build various sized atoms and since these tachyonic neutrinos are directly involved in the mechanical process of manifesting gravity, this mechanism of gravity may be called a conceptual resurrection of quantum gravity from the perspective of tachyonic magnetic monopole background neutrinos.

7. Push Theory of Gravity

As it may have become obvious by now, we hypothesize that the background tachyonic magnetic monopole neutrinos are the cause of gravity as well as inertial mass. The impact by the background tachyonic magnetic monopole neutrinos on

hadrons represent itself as force which is the cause of acceleration, only if the beam of TMMN (tachyonic magnetic monopole neutrinos) is one directional. However, in reality, the TMMN flux is isotropic and homogenous; consequently, all the forces are canceled and there is no net acceleration for a macroscopic object in flat space time. However, if one can block the flow of the TMMN flux from one direction from the test object, the direction and magnitude of the blocked TMMN flux will define the gravity force and its direction. Alternatively, in the case of directional impact, one can create a beam of TMMN flux and point it directly to an object to cause an impact.

The flat space-time model of general relativity essentially describes a space filled with a uniform density of tachyonic magnetic monopole neutrinos without any massive gravitating object nearby to disturb the isotropic uniformity of the density of the TMMN. In the presence of massive gravitational objects, the spacetime is warped because the distribution of the tachyonic magnetic monopole background neutrinos is not homogeneous owing to the blockage of the free passage of these neutrino particles, which causes a distortion of the density profile in the nearby space of these background particles. Because the density of hadrons is determined by the internal quarks and gluons, it is unlikely that the strong compressive force exerted by the background neutrinos could make it denser than that of the typical hadrons. This reasoning makes it highly unlikely that a blackhole with near-infinite mass density can be formed in the universe. If the hadronic structure is determined by quantum chromodynamics, the force of gravity near the center of the black hole will be very close to that caused by the density of the hadrons and nothing more. Therefore, the valid range of gravity caused by tachyonic magnetic monopole background (anti)neutrinos is outside the realm of the hadronic structure.

8. Filament Structure of Far Away Galaxies

Another interesting fact is the observation of the far outside of the universe, which has distinctive filament patterns in its structure. This can be explained by using the tachyonic magnetic monopole background neutrinos because, for obvious reasons, the space between the two massive gravitational masses suffers from a lack of neutrino density along the path in between, and this linear domain of the universe can be filled with a more massive object. This accumulation of mass adds to the lack of neutrino density and attracts more mass particles, eventually forming a filament structure of the gigantic nuclear fusion reaction. The key to understanding the matter distribution in the universe is that the low-density region of the background tachyonic magnetic monopole neutrino becomes the gravitational center/attractor where hadronic particles tend to migrate toward and cause nuclear fusion reactions to brighten the surrounding region to be visible from the earth. In this respect, it is possible to engineer the density of the local tachyonic magnetic monopole neutrinos to navigate the universe because, after all, it boils down to the control of the local magnetic field density that determines its possi-

bility. If the vehicle has the capability of creating a low-density magnetic field focused in front of the vehicle and a high-density magnetic field spread out behind, using three columns of strong magnetic field that can be focused in the longitudinal direction, it will continuously follow the trajectory toward the low-density background neutrino space because the low-density region of the neutrino density moves further away as the vehicle moves forward. Considering that the recent development of room-temperature superconductors, thereby creating and manipulating strong magnetic fields, is easily manageable, the prospect of this project looks much brighter.

9. Possible Existence of the Universe Composed of Opposite Polarity of Electric and Magnetic Charges

This is a philosophical conjecture rather than a physical reality. If the universe is symmetric for everything, as we expect it to be, we have to come to the question of why our universe is made of a combination of negatively charged electrons and the north pole magnetic monopole, that is, electrons and electron neutrinos. It is totally arbitrary, and nothing dictates that the universe must be made this way. This means that there is nothing that will prevent the existence of the universe made of positrons, antiprotons, and south pole magnetic monopole neutrinos (anti-neutrinos). No universal law prohibits the existence of such a universe. If such a universe does exist, according to CPT (charge-parity-time) invariance, this universe must have the time going backward relative to ours. This subject is beyond the scope of the present discussion in this paper, but it is certainly a very tantalizing issue that needs to be investigated in the future.

10. Conclusions

Any valid theory of physics regarding the workings of the universe must have connections with other known and experimentally verified theories. This is because everything is related to each other and nothing is isolated in the universe. It was not our original intention to devise a theory of gravity in the beginning, when we ventured to investigate and measure the magnetic monopole charge of neutrinos. However, it became obvious that these background magnetic monopole tachyonic neutrinos cannot be separated from gravity. If these particles can cause momentum in their model to explain the quantum phenomenon, it is natural to suspect that gravity must be involved in this mechanism also because Newton's first law of motion explicitly states the property of inertia. On this subject, not only Newton himself, but many other researchers have deeply delved into this study, suggesting that gravity could be a push effect. We conclude that this is exactly what gravity is from the perspective of tachyonic magnetic monopole background neutrinos.

The above article confirms that the special relativistic effect creates a relative additional vacuum in the background density of tachyonic magnetic monopole neutrinos around the rotating objects, which increases the mass of the particle

because of the bouncing-off effect of the magnetic monopole neutrinos by hadronic particles. After all, the local density of the background neutrinos affects gravity either by special relativity or by the hadronic mass itself. To navigate the universe without using rocket propulsion, it is necessary to control the background density of tachyonic magnetic monopole neutrinos around the craft that navigates through space. The authors would like to thank the Tachyonics Institute of Technology for supporting this work.

Conflicts of Interest

The author declares that he has no affiliation with or involvement with any other organization or entity with any financial interest in the subject matter or materials discussed in this manuscript.

References

[1] Weinberg, S. (1967) A Model of Leptons. *Physical Review Letters*, **19**, 1264-1266. https://doi.org/10.1103/physrevlett.19.1264

[2] Dau, W.D. (1983) UA1 Results from pp Collisions at AT $\sqrt{s} = 540$ GeV . https://articles.adsabs.harvard.edu/full/1983ICRC...12...71D

[3] ATLAS Collaboration (2012) Observation of a New Particle in the Search for the Standard Model Higgs Boson with the ATLAS Detector at the LHC. *Physics Letters B*, **716**, 1-29. https://cds.cern.ch/record/1471031/files/plb-716-1.pdf

[4] Gell-Mann, M. and Low, F.E. (1954) Quantum Electrodynamics at Small Distances. *Physical Review*, **95**, 1300-1312. https://doi.org/10.1103/physrev.95.1300

[5] Hooft, G. and Veltman, M. (1972) Regularization and Renormalization of Gauge Fields. *Nuclear Physics B*, **44**, 189-213. https://doi.org/10.1016/0550-3213(72)90279-9

[6] Yukawa, H. (1955) On the Interaction of Elementary Particles. I. *Progress of Theoretical Physics Supplement*, **1**, 1-10. https://doi.org/10.1143/ptps.1.1

[7] Ramond, P. (1980) Field Theory: A Modern Primer. https://www.phys.ufl.edu/~ramond/Chapter1_CUP.pdf

[8] Gross, D.J. and Wilczek, F. (1973) Ultraviolet Behavior of Non-Abelian Gauge Theories. *Physical Review Letters*, **30**, 1343-1346. https://doi.org/10.1103/physrevlett.30.1343

[9] Barnes, A. and Scargle, J.D. (1975) Improved Upper Limit on the Photon Rest Mass. *Physical Review Letters*, **35**, 1117-1120. https://doi.org/10.1103/physrevlett.35.1117

[10] Hawking, S.W. (1974) Black Hole Explosions? *Nature*, **248**, 30-31. https://doi.org/10.1038/248030a0

[11] Bjorken, J.D. and Drell, S.D. (1964) Relativistic Quantum Mechanics. McGraw-Hill. https://ivlabs.github.io/resources/physics/books/Relativistic%20Quantum%20Fields%20by%20James%20D.%20Bjorken,%20Sidney%20D.%20Drell.pdf

[12] Eichten, E., Gottfried, K., Kinoshita, T., Kogut, J., Lane, K.D. and Yan, T. (1976) Spectrum of Charmed Quark-Antiquark Bound States. *Physical Review Letters*, **36**, 1276. https://doi.org/10.1103/physrevlett.36.1276

[13] LaRue, G.S., Fairbank, W.M. and Hebard, A.F. (1977) Evidence for the Existence of Fractional Charge on Matter. *Physical Review Letters*, **38**, 1011-1014. https://doi.org/10.1103/physrevlett.38.1011

[14] Newton, I. (1686) 1686 Isaac Newton Philosophiae Naturalis Principia Mathematica. (Newton's Personally Annotated 1st Edition). https://archive.org/details/1686-newton-principia-1ed

[15] Einstein, A. (1905) Ist die Trägheit eines Körpers von seinem Energieinhalt abhängig? [Does the Inertia of a Body Depend Upon its Energy-Content?]. *Annalen der Physik*, **323**, 639-641. https://doi.org/10.1002/andp.19053231314

[16] Mach, E. (1960) The Science of Mechanics: A Critical and Historical Account of Its Development. Open Court Publishing Co. LCCN 60010179.

[17] Einstein, A. (1915) Die Feldgleichungen der Gravitation. Sitzungsberichte der Königlich Preußischen Akademie der Wissenschaften (Berlin), 844-847. https://ui.adsabs.harvard.edu/abs/1915SPAW.....844E/abstract

[18] Misner, C.W., Thorne, K.S. and Wheeler, J.A. (1973) Gravitation. Freeman, 991 p. https://physicsgg.me/wp-content/uploads/2023/05/misner_thorne_wheeler_gravitation_freema.pdf

[19] von Laue, M. (1921) Die relativitätstheorie, University of Michigan Library, 203-204.

[20] Weinstein, D.H. (1971) Ehrenfest's Paradox. *Nature*, **232**, 548-548. https://doi.org/10.1038/232548a0

[21] Phipps, T.E. (1974) Kinematics of a "Rigid" Rotor. *Lettere al Nuovo Cimento*, **9**, 467-470. https://doi.org/10.1007/bf02819912

[22] Jeong, E.J. (1999) Non-Newtonian Force Experienced by Gravitational Dipole Moment at the Center of the Two Mass Pole Model Universe. *Physica Scripta*, **59**, 339-343. https://doi.org/10.1238/physica.regular.059a00339

[23] Thirring, H. (1918) Über die Wirkung rotierender ferner Massen in der Einsteinschen Gravitationstheorie. *Physikalische Zeitschrift*, **19**, 33.

[24] Cohen, J.M. and Sarill, W.J. (1970) Centrifugal Force and General Relativity. *Nature*, **228**, 849-849. https://doi.org/10.1038/228849a0

[25] Bass, L. and Pirani, F.A.E. (1955) XCVI. On the Gravitational Effects of Distant Rotating Masses. *The London, Edinburgh, and Dublin Philosophical Magazine and Journal of Science*, **46**, 850-856. https://doi.org/10.1080/14786440808561237

[26] Cohen, J.M., Sarill, W.J. and Vishveshwara, C.V. (1982) An Example of Induced Centrifugal Force in General Relativity. *Nature*, **298**, 829-829. https://doi.org/10.1038/298829a0

[27] Pietronero, L. (1973) The Mechanics of Particles Inside a Rotating Cylindrical Mass Shell. *Annals of Physics*, **79**, 250-260. https://doi.org/10.1016/0003-4916(73)90291-1

[28] Navarro, J.F., Frenk, C.S. and White, S.D.M. (1996) The Structure of Cold Dark Matter Halos. *The Astrophysical Journal*, **462**, 563. https://doi.org/10.1086/177173

[29] Xiao, Y.M., *et al.* (1991) Gravity Probe B: III. The Precision Gyroscope. *Proceedings of the Sixth Marcel Grossmann Meeting on General Relativity*, Kyoto, 394-398. https://einstein.stanford.edu/content/sci_papers/papers/XiaoYM_1991_24.pdf

[30] Cohen, C.E., Keiser, G.M. and Parkinson, B.W. (1992) Estimation of Gyroscope Polhode Motion Using Trapped Magnetic Flux. *Journal of Guidance, Control, and Dynamics*, **15**, 152-158. https://doi.org/10.2514/3.20813

[31] Everitt, C.W.F., DeBra, D.B., Parkinson, B.W., Turneaure, J.P., Conklin, J.W., Heifetz, M.I., *et al.* (2011) Gravity Probe B: Final Results of a Space Experiment to Test General Relativity. *Physical Review Letters*, **106**, Article ID: 221101. https://doi.org/10.1103/physrevlett.106.221101

[32] https://einstein.stanford.edu/Media/Polhode_motion-animation.html

[33] Dirac, P.A.M. (1931) Quantized Singularities in the Electromagnetic Field. *Proceedings of the Royal Society of London A*, **133**, 60-72. http://users.physik.fu-berlin.de/~kleinert/files/dirac1931.pdf https://doi.org/10.1098/rspa.1931.0130

[34] Hooft, G. (1974) Magnetic Monopoles in Unified Gauge Theories. *Nuclear Physics B*, **79**, 276-284. https://doi.org/10.1016/0550-3213(74)90486-6

[35] Polyakov, A.M. (1974) Particle Spectrum in the Quantum Field Theory. *JETP Letters*, **20**, 194-195. https://inspirehep.net/literature/90679

[36] Chodos, A., Hauser, A.I. and Alan Kostelecký, V. (1985) The Neutrino as a Tachyon. *Physics Letters B*, **150**, 431-435. https://doi.org/10.1016/0370-2693(85)90460-5

[37] Recami, E. (1978) Tachyons, Monopoles and Related Topics. *Proceedings of the First Session of the Interdisciplinary Seminars on "Tachyons and Related Topics"*, Erice, 1-15 September, 1978, 285.

[38] Bilaniuk, O.M.P., Deshpande, V.K. and Sudarshan, E.C.G. (1962) "Meta" Relativity. *American Journal of Physics*, **30**, 718-723. https://doi.org/10.1119/1.1941773

[39] Bilaniuk, O. and Sudarshan, E.C.G. (1969) Particles Beyond the Light Barrier. *Physics Today*, **22**, 43-51. https://doi.org/10.1063/1.3035574

[40] Simpson, J.J. (1982) Third Workshop on Grand Unification. Birkhäuser, 258 p. https://doi.org/10.1007/978-1-4612-5800-1

[41] Pati, J.C. and Salam, A. (1974) Lepton Number as the Fourth "Color". *Physical Review D*, **10**, 275-289. https://doi.org/10.1103/physrevd.10.275

[42] Polchinski, J. (1998) String Theory. Cambridge University Press. https://doi.org/10.1017/cbo9780511816079

[43] Steyaert, J.J. (1988) The Neutrino as a Tachyonic Non-Charged Light Magnetic Monopole? In: Klapdor, H.V. and Povh, B., Eds., *Neutrino Physics*, Springer, 159-162. https://doi.org/10.1007/978-3-642-73679-7_16

[44] Loureiro, A., Cuceu, A., Abdalla, F.B., Moraes, B., Whiteway, L., McLeod, M., *et al.* (2019) Upper Bound of Neutrino Masses from Combined Cosmological Observations and Particle Physics Experiments. *Physical Review Letters*, **123**, Article ID: 081301. https://doi.org/10.1103/physrevlett.123.081301

[45] Khan, T.A., Kadir, K., Alcm, M., Fchiihid, Z. and Mazliham, M.S. (2017) International Conference on Engineering Technology and Technopreneurship (ICE2T).

[46] http://www.sciencelearn.org.nz

[47] Salat, C. and Junge, A. (2010) Dielectric Permittivity of Fine-Grained Fractions of Soil Samples from Eastern Spain at 200 MHz. *Geophysics*, **75**, J1-J9. https://doi.org/10.1190/1.3294859

[48] Finlay, C.C., Maus, S., Beggan, C.D., Bondar, T.N., Chambodut, A., Chernova, T.A., *et al.* (2010) International Geomagnetic Reference Field: The Eleventh Generation. *Geophysical Journal International*, **183**, 1216-1230. https://doi.org/10.1111/j.1365-246x.2010.04804.x

[49] Abundance of Elements in the Earth's Crust and in the Sea. https://www.scribd.com/document/667442939/Abundance-of-Elements-in-the-Earth-s-Crust-and-in-the-Sea

[50] Jackiw, R. (2002) Dirac's Magnetic Monopoles (Again). arXiv: hep-th/0212058.

[51] Bialynicki-Birula, I. and Bialynicka-Birula, Z. (1971) Magnetic Monopoles in the Hydrodynamic Formulation of Quantum Mechanics. *Physical Review D*, **3**, 2410-2412. https://doi.org/10.1103/physrevd.3.2410

[52] Robertson, R.G.H., Bowles, T.J., Stephenson, G.J., Wark, D.L., Wilkerson, J.F. and Knapp, D.A. (1991) Limit on $\bar{\nu}_e$ Mass from Observation of the β Decay of Molecular Tritium. *Physical Review Letters*, **67**, 957-960. https://doi.org/10.1103/physrevlett.67.957

[53] Uggla, C. (2006) Spacetime Singularities. https://www.einstein-online.info/en/spotlight/singularities/

[54] Lineweaver, C.H. and Davis, T.M. (2005) Misconceptions about the Big Bang. *Scientific American*, **292**, 36-45. https://doi.org/10.1038/scientificamerican0305-36

[55] Einstein, A., Podolsky, B. and Rosen, N. (1935) Can Quantum-Mechanical Description of Physical Reality Be Considered Complete? *Physical Review*, **47**, 777-780. https://doi.org/10.1103/physrev.47.777

[56] IceCube Collaboration (2013) Evidence for High-Energy Extraterrestrial Neutrinos at the IceCube Detector. *Science*, **342**, Article ID: 1242856. https://doi.org/10.1126/science.1242856